Methanol synthesis through CO2 capture and hydrogenation: Thermal integration, energy performance and techno-economic assessment

Methanol synthesis through CO_2 capture and hydrogenation: thermal integration, energy performance and techno-economic assessment

Patrizio Battaglia[2], Giulio Buffo*[,1], Domenico Ferrero[1], Massimo Santarelli[1], Andrea Lanzini[1]

[1] Dipartimento Energia "Galileo Ferraris", Politecnico di Torino – C.so Duca degli Abruzzi 24, 10129 Torino (Italy)

[2] Dipartimento di Ingegneria Meccanica e Aerospaziale, Politecnico di Torino – C.so Duca degli Abruzzi 24, 10129 Torino (Italy)

*Corresponding author: giulio.buffo@polito.it

ABSTRACT

This work assesses the opportunity of using "green" methanol (MeOH) produced from renewable electricity as a vector for the decarbonization of chemical process industry. We developed a comprehensive process model to simulate all the relevant sections for the conversion of 1.25 t/h of captured CO_2 from a coal-fired power plant to methanol, using "green" hydrogen via water electrolysis. We applied the pinch analysis methodology for an improved thermal management of the integrated carbon capture, electrolysis and methanol synthesis plant. A network of recovery heat exchangers was designed with the pinch analysis methodology, allowing a thermal energy saving of 4.59 MW, with a net reduction of heating and cooling demands by 81% and 47%, respectively, and an improvement of the global efficiency of the plant from 26.74% to 37.22. We followed a bottom-up approach for the techno-economic assessment, defining a confidence range for the main indicators of system economic viability. We assessed their sensitivity to the cost of electricity from seven renewable energy sources and to the option of selling oxygen produced by water electrolysis, in three different cost scenarios (1-optimistic, 2-realistic, 3-pessimistic). The estimated values of the cost of methanol (COM) span from a maximum range of 2624-2706 €/t (in the case of concentrated solar power) to a minimum of 565-647 €/t (hydropower with highest valorization of electrolytic oxygen), hence resulting in line with the future trends of methanol market price (400-800 €/t) in five of the considered configurations. We have finally estimated the levelized cost of methanol (LCOM) ensuring an internal rate of return ranging from 0 to 10% for each of the techno-economic scenarios identified. Assuming 10% as the target, LCOM in case of hydropower as renewable energy source spans from 874 to 1356 €/t, hence close to the future market price of MeOH with margin of improvement (655-1135 €/t) in case of lower costs of electric energy.

Keywords: carbon capture and utilization; electrolysis; CO_2 hydrogenation; methanol synthesis; energy performance; techno-economic assessment.

Highlights

- Comprehensive process model of a large-scale green power-to-methanol system
- Thermal integration saves 4.59 MW reducing the heating demand by 81%
- We assessed the sensitivity on system economic profitability
- The costs of green and fossil methanol compete in 5 of the studied scenarios
- A production cost of methanol of 874 €/t ensures a 10% internal rate of return

---

List of abbreviations

BEC	Bare Erected Cost
CEPCI	Chemical Engineering Plant Cost Index
COM	Cost of methanol
EBIT	Earnings before interest and taxes
EBITDA	Earnings before interest, taxes, depreciation and amortization
EPCC	Engineering, procurement, and construction cost
FCF	Free Cash Flow
HHV	Higher heating value
IRR	Internal rate of return
LCOE	Levelized cost of electricity
LCOM	Levelized cost of methanol
LHV	Lower heating value
MEA	Monoethanolamine
MeOH	Methanol
NPV	Net present value
OPEX	Operating cost
PBP	Payback period
PC	Process Contingencies
PtX	Power-to-X
RES	Renewable Energy Sources

SPECCA	Specific plant energy consumption for CO_2 avoided
TIC	Total Invested Cost
TOC	Total Overnight Cost
TPC	Total Plant Cost

List of symbols

$\boldsymbol{A}$	-	Amortization of the invested capital
$\boldsymbol{B_{1\text{-}2}}$	-	Constants for bare module cost (heat exchangers, process vessels and pumps)
$\boldsymbol{C_{BM,main}}$	*€*	Bare module cost of main components
$\boldsymbol{C_{BM,tot}}$	*€*	Total bare module cost
$\boldsymbol{C_{BM,WE}}$	*€*	Total bare module cost of the electrolyzer
$\boldsymbol{\tilde{c}_{BM,WE}}$	*€/kW*	Total specific bare module cost of the electrolysis module
$\boldsymbol{c_p}$	*kJ/kg/K*	Specific heat capacity
$\boldsymbol{C_p^0}$	*€*	Purchased cost of a component (carbon steel, p = 1 bar)
$\boldsymbol{E_{el_{CO2}}}$	*MWh/y*	Annual electric consumption of the carbon capture section
$\boldsymbol{E_{el_{sys}}}$	*MWh/y*	Annual electric consumption of the system
$\boldsymbol{F_{BM}}$	-	Bare module factor
$\boldsymbol{F_M}$	-	Material factor
$\boldsymbol{F_P}$	-	Pressure factor
$\boldsymbol{i}$	-	Discount rate
$\boldsymbol{k}$	*year*	Years since the investment
$\boldsymbol{K_{1\text{-}3}}$	-	Parameters of the cost function for the estimation of C_P^0
$\boldsymbol{\dot{m}}$	*kg/s*	Mass flow rate
$\boldsymbol{m_{CO2}}$	*kt/y*	Annual amount of carbon dioxide captured and converted
$\boldsymbol{m_{MeOH}}$	*t/y*	Annual production of methanol
$\boldsymbol{n}$	-	Cost exponent
$\boldsymbol{n_{life}}$	*years*	Plant lifetime (25 years)
$\boldsymbol{OC}$	*€/y*	Operating cost in annual cash flow
$\boldsymbol{p}$	*bar*	Absolute pressure
$\boldsymbol{P_{WE}}$	*kW*	Nominal size of the electrolysis stack
$\boldsymbol{\dot{Q}_{cooling}}$	*kW*	Demand of external cooling energy
$\boldsymbol{\dot{Q}_{heating}}$	*kW*	Demand of external heating energy
$\boldsymbol{q_{reb}}$	kJ/g_{CO2}	Specific regeneration heat duty of the solvent in carbon capture section

$\boldsymbol{Q_{th_{CO2}}}$	*MWh/y*	Annual thermal consumption of the carbon capture section
$\boldsymbol{Q_{th_{sys}}}$	*MWh/y*	Annual thermal consumption of the system
$\boldsymbol{R}$	*€*	Revenue in the annual cash flow
$\boldsymbol{S}$	*variable*	Characteristic size of a component
$\boldsymbol{T}$	*°C*	Temperature
$\boldsymbol{Tax}$	*€*	Corporate income tax rate
$\boldsymbol{V_{H2O}}$	km^3/y	Annual water consumption

Greek symbols

$\boldsymbol{\alpha}$	-	Solvent CO_2 loading
$\boldsymbol{\Delta T_{min}}$	*°C*	Minimum temperature difference between hot and cold fluids in pinch analysis
$\boldsymbol{\eta_{gl}}$	-	Global efficiency of the Power-to-MeOH system
$\boldsymbol{\Psi}$	-	CO_2 removal rate

1. Introduction

Since the first Industrial Revolution, fossil fuels have been the main source of primary energy in several sectors of economy such as power plants and industry and they will still probably maintain an important role in the current century [1]. However, the increasing and accelerating emission of greenhouses gases such as carbon dioxide (CO_2) from the process of combustion [2] has already broken the equilibrium between natural sinks and sources in the so-called "carbon cycle". Global warming and climate change concerns have recently furthered political efforts to avoid the worst effects of this excess of anthropogenic CO_2 in the atmosphere. Signed in 2015 by 196 countries, the Paris Agreement [3] aims to hold global temperature well below 2 °C above pre-industrial average level, increasing the ability to adapt to the adverse impacts of climate change. To this end, carbon emissions to the atmosphere must peak as soon as possible so that they can decrease later until achieving a neutral balance. In a recent report [4], the Intergovernmental Panel on Climate Change states that limiting global warming to 1.5 °C can be implemented through different mitigation measures: lowering energy and resource intensity, increasing the rate of decarbonization and promoting carbon capture processes.

Carbon capture would be an interim strategy for the stabilization of the emissions due to the use of fossil fuels, but also a long-term solution for the reuse of carbon. In this context, captured CO_2 could be exploited as a raw molecule for the long-term storage of power from RES (renewable energy sources) into chemical form following the Power-to-X (PtX) scheme [5] through reaction with hydrogen produced via different processes, such as water electrolysis. The yielded synthetic gas can be upgraded to many "X" gaseous/liquid fuels and chemicals characterized by high

market value and dispatchability [6]. In particular, future economy will strongly rely on liquid fuels/chemicals due to their capability of storing and displacing remarkable amounts of energy thanks to their high energy density [7].

Methanol (MeOH) is a promising liquid energy carrier with potential use in several applications, either as a chemical or a fuel or as a platform molecule for the synthesis of heavier alcohols, dimethyl ether, gasoline and more complex chemicals, such as olefins [8]. Synthesizing methanol from captured CO_2 and green hydrogen is a valuable opportunity for the decarbonization of chemical process industry and economic sector currently relying on fossil methanol. Table 1 reports the main thermodynamic properties of methanol.

Table 1 - Physical properties of methanol

Molecular weight (g/mol)	32.04	**Latent heat of vaporization (25 °C, kJ/mol)**	37.43
Critical temperature (°C)	239	**Vapor pressure (25 °C, bar)**	0.1696
Critical pressure (bar)	79.5	**LHV (25°C and 1.013 bar, kJ/mol)**	638.1
Freezing point (1.013 bar, °C)	-97.6	**HHV (25°C and 1.013 bar, kJ/mol)**	726.1
Boiling point (1.013 bar, °C)	64.6	**Auto-ignition temperature (°C)**	470

With a global demand of 60-70 Mt/year in 2015 expected to increase to 190 Mt/year by 2030 [9], more than 80% of methanol production is based on steam reforming of natural gas. However, this process is associated with huge greenhouse gas emissions [10]. The synergy of electrochemical synthesis of hydrogen and its thermocatalytic reaction with captured CO_2 provides alternative pathways for the production of synthetic methanol [11], such as a 1-step direct hydrogenation of CO_2 or a reverse water-gas shift reaction followed by methanol synthesis (as in the case of the CAMERE process, [12]). The overall reduction of greenhouse gas emissions of these pathways with respect to its fossil counterpart is effective only if energy supplied and chemical reactants are characterized by low carbon intensity. Hence, the market for conversion of CO_2 into "green" methanol is strictly driven by the diffusion and storage of RES in chemical form [9]. In fact, the access to clean energy supply and low-cost renewable hydrogen is the main barrier to the commercialization of CO_2-to-MeOH processes, together with the low efficiency of available catalysts [9,13]; however, pilot programs are in place to investigate these processes and mitigate the associated techno-economic risks [9].

For instance, the "Liquid Sunshine" project in China spans over 50 years and progressively explores the vision of transporting RES throughout the world in the form of methanol [14,15]. Starting from the demonstration of technologies employing hard coal as a raw feedstock of carbon, the project will gradually introduce "sunshine" for electricity supply through PV panels and biomass as carbon source to make the storage and dispatchment chain

fully sustainable and cost-effective [16]. Concluded in 2019, the European MefCO_2 project [17] investigated the techno-economic feasibility of converting renewable H_2 and captured CO_2 to methanol and demonstrated it with a 7.2-t/day CO_2 capture and conversion plant in a coal-fired power station in Germany [18,19]. In Iceland, a commercial-size CO_2-to-MeOH plant has been operating since 2012 producing 4 kt/y of methanol [20,21]. CO_2 is extracted as a co-product together with steam in a geothermal power plant and captured for reaction in a heterogeneous catalytic reactor with H_2 produced via water electrolysis fed by low-carbon grid electricity [22].

Pushed by the increasing momentum of methanol option for Power-to-Fuels storage, a wide range of literature has recently focused on the study of Power-to-MeOH systems to meet the urgencies of RES diffusion and multi-sectorial decarbonization of economy. Models were developed to simulate the operation of the whole Power-to-MeOH system [10,11,23,24] and to assess thoroughly the techno-economic feasibility [25–27] and the emission savings [28] of the process in different operational scenarios. However, although the sustainability of the process has been discussed from different points of view, little attention has been paid to the potential benefit of heat integration of the different sections of a Power-to-MeOH system on energy performance as well as to the sensitivity of the cost of MeOH to the main economic parameters, such as the electric energy price and the contingencies in the definition of the invested capital.

This work presents a comprehensive model of a full Power-to-MeOH system for the industrial production of "green" methanol through direct hydrogenation of CO_2 captured from a coal-fired power plant (Section 2). Carbon capture system (Section 3.1.1) through amine scrubbing was first modelled starting from real experimental data, validated using the results of the pilot plant designed by Notz et al. [29] as reference and then scaled up to treat a larger flue gas volume. The methanol synthesis (Section 3.1.3) through reaction with hydrogen produced by an alkaline electrolyzer (Section 3.1.2) was modelled taking the cue from the model developed in [30]. In Section 3.2 we highlight the importance of thermal integration of the different sections of the process, so to reduce the thermal needs of the plant. The consumed streams of energy and raw materials resulting from the simulations (Section 4.1) were used to assess the main energy and environmental performance indicators of the Power-to-MeOH system (Section 4.2). Adopting a bottom-up estimation of the total overnight cost (TOC) described in Section 3.3, we computed the levelized cost of MeOH in different scenarios of power supply, providing a confidence range according to reasonable hypotheses on TOC definition and its sensitivity to electric energy price (Section 4.3). Finally, we determined the main energy and economic key performance indicators of the modelled Power-to-MeOH system to assess its viability and prove its economic competitiveness as an option for the decarbonization of methanol industry and market in the considered scenarios.

2. Layout of the plant and case-study

Figure 1 presents the scheme of the studied Power-to-MeOH system and its subdivision in three sections:

- Water splitting into hydrogen and oxygen through alkaline electrolyzers;
- Carbon capture with amine-based liquid solvents;
- Synthesis and purification of methanol through direct hydrogenation of captured CO_2.

As a sustainable alternative to the well-established process of steam methane reforming, we studied the opportunity of using "green" methanol produced from RES as a value-added feedstock for a fully decarbonized chemical process industry. To this end, water electrolysis is fed by energy certified as produced from renewable sources, such as the production of a renewable energy cluster, grid curtailment (i.e. RES overproduction) or low-carbon electric energy purchased from the grid in locations with a very high penetration of RES. The input of renewable electricity is assumed to be constantly available for water electrolysis; the coupling of the system with a real RES availability profile would require also a system of buffers for the raw gases (H_2 and, possibly, CO_2) suitably sized through a time-resolved model. This is beyond the scope of this paper, in which we developed a model for the nominal operation of the integrated Power-to-MeOH scheme to assess its feasibility from energy and economic standpoints. The study focuses on the production of methanol at a commercial scale (1 m^3/h of methanol, i.e. about 800 kg/h) and the size of water electrolysis and carbon capture sections was selected in order to feed the methanol synthesis section with sufficient flows of hydrogen and CO_2 captured. We set the size of water electrolysis section equal to 10 MW, hence producing a constant flow rate of 1.9 kNm^3/h of hydrogen (specific consumption of 5.4 kWh/Nm^3_{H2}) at a pressure of 10 bar. Pure electrolytic hydrogen (99.7%$_v$ without auxiliary purification equipment) is then compressed for the synthesis of methanol; oxygen is either vented in the base scenario or sold.

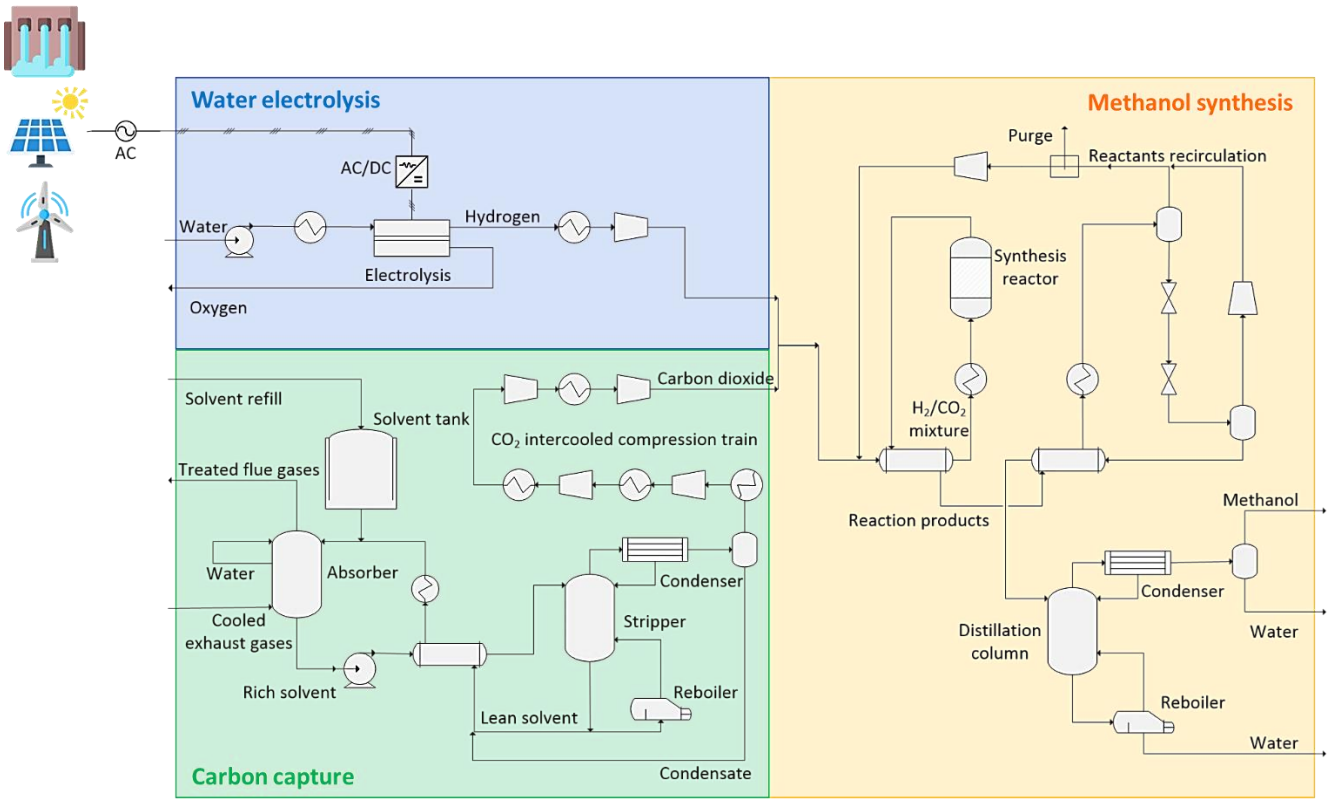

Figure 1 - Layout of the Power-to-MeOH system

In the carbon capture section, a traditional two-column system captures 632 Nm^3/h of CO_2 (99.7%$_w$ purity) from 7.9 kNm^3/h of exhausts from a coal-fired power plant through an amine scrubbing process with an aqueous solution of monoethanolamine (MEA), considered as the most mature technology available in the market. The choice of a coal-fired plant as the source of CO_2 for methanol synthesis is due to the availability of real data of the pilot plant for carbon capture from the exhausts of coal combustion reported in Ref. [29] for the steady-state model of this section. Furthermore, burning hard coal produces exhausts with an intermediate composition between highly concentrated sources of CO_2 (e.g., biogas upgrading) and diluted point-like streams (e.g., exhausts in gas-fired power plant), hence representing an average source of carbon. Moreover, the elemental composition of exhausts from coal combustion is very close to that of the exhausts from the incineration of municipal solid wastes, an interesting source of CO_2 for applications in the framework of circular economy. CO_2 absorption occurs in the absorption column where the solvent flows downwards, in counter-current with the gas mixture coming from the bottom: the CO_2-poor gas mixture leaves the top of the absorber. The CO_2-rich solvent leaving the absorber from the bottom is pumped and heated up and flows downwards in the desorption column: the solvent is thermally regenerated by a reboiler, so CO_2 is stripped and leaves the column top. The lean solvent recirculates back to the

absorber through the recovery heat exchanger with a refill in case of leakages for entrainment in the columns and evaporation.

This layout is the most adopted for the capture of CO_2 with liquid solvents through physisorption (e.g., pressurized water scrubbing) and/or chemisorption. Amine scrubbing with MEA represents the state-of-art of chemisorption of CO_2. The high specific solvent circulation rate and the energy penalty for solvent regeneration make this solution a technologic baseline for carbon capture. Research is currently investigating alternative techniques such as blending or even replacing amines with conventional or functionalized ionic liquids [31] to reduce regeneration heat duty and improve reaction kinetics, calcium looping for high-temperature processes [32], low-temperature adsorbents (e.g., zeolites, MOFs, activated carbons etc.) [33], just to name a few. These promising routes endeavor to raise the energy performance and reduce the costs of carbon capture with respect to the state-of-art technology that is studied in this work.

Captured carbon dioxide flows through an intercooled compression train and mixes with electrolytic hydrogen from water electrolysis section. The pressurized H_2/CO_2 feed (65 bar) is heated up to 250 °C and fed to the reactor for methanol synthesis through direct hydrogenation of CO_2: the state of art consists of a reactor equipped with copper-based catalyst – $CuO/ZnO/Al_2O_3$ (CZA) – operating in the pressure range of 50-100 bar [34,35].

Concerning the catalyst, the use of CZA is the most common option for CO_2 hydrogenation as well as for the traditional methanol synthesis from CO-rich syngas, as this type of catalyst is very active for both processes.The choice of the operating pressure is due to the Cu-based catalyst, which requires a pressure range of 5-10 MPa to obtain a good methanol selectivity (above 50%) in the presence of CO_2 and H_2, while at lower pressure the rate of formation of CO by reverse water gas shift becomes higher (1-3 orders of magnitude) than that of methanol and thus the resulting CH_3OH selectivity is extremely low [36]. Several novel catalyst materials are under development with the aim to obtain high methanol selectivity at lower pressure, thus reducing the complexity (and cost) of the synthesis plant. Liao et al. [36] investigated a Pd-Zn catalyst for CO_2 hydrogenation that at 2 MPa showed a CH_3OH selectivity of 70% compared to 10% over an industrial Cu catalyst. Other works investigated less precious materials, as NiGa [37] or CoGa catalysts [38]. Other approaches involve the improvement of Cu/ZnO using zeolites to add acidic properties and increase reactivity or their confinement in MOFs [19].

The gas mixture leaving the reactor undergoes some steps of pressure reduction and temperature swing for flash separation of gases other than methanol, then a distillation column separates the methanol and a final mechanical separator raises the purity of the produced stream to 99.9% of CH_3OH.

3. Methodology

This section of the paper describes the methodology developed to model the steady-state operation of the three sections of the system (Section 3.1) and their thermal integration with the pinch analysis approach (Section 3.2) in the considered case study. A thorough description of the plant revenue accounting with the cash flow analysis methodology is provided in Section 3.3, while Section 3.4 presents the indicators of the energy and economic performance of the Power-to-MeOH system. A list with a description of the components in the different sections and their corresponding ID is reported in Table S.1 in the Supplementary Material.

3.1. Steady-state process model

Mass and energy balances and thermodynamic transformations of the operating streams in each of the three sections in Figure 1 were developed using the commercial process simulator Aspen Plus™. As general assumptions for all the modeled sections, 75% isentropic efficiency was set for each compression stage and internal pressure drops were neglected for the circulation pumps and heat exchangers.

3.1.1. Water electrolysis

This section models the production of the necessary hydrogen for the downstream synthesis of methanol. Water was fed to an equilibrium reactor, a component available in Aspen Plus™ used to reproduce the constant operation at nominal point of 10.26 MW of the alkaline electrolyzer, the most mature, available and affordable technology for low-temperature water electrolysis at commercial scale [39]-[40]. Tap water at p =1 atm and T=15°C (stream 101 in Figure 2) was pumped and heated to feed the electrolyzer at 70 °C and 10 bar.

Feedwater was dissociated within the electrolyzer according to the reactions listed in Table 2 in a constant flow rate of 1.9 kNm^3/h of H_2 (assuming a specific energy consumption for electrolysis of 5.4 kWh/Nm^3_{H2} [41]) and 0.95 kNm^3/h of oxygen, split through a separator that simulates in the model the electrolyte interposed between the two electrodes of a real alkaline cell.

Table 2 - Chemical reactions employed in the model of the water electrolysis section

Reaction	Type
1) $2\ H_2O + 2\ e^- \leftrightarrow H_2 + 2\ OH^-$	Equilibrium
2) $2\ OH^- \leftrightarrow H_2O + ½\ O_2 + 2\ e^-$	Equilibrium
3) $H_2O \leftrightarrow ½\ O_2 + H_2$ (overall)	Equilibrium

Excess water at the outlet was recirculated back to the reactor (i.e., to the stack inlet). Hydrogen was produced (stream 105) at high purity (99.7%) and pure oxygen (stream 104) is vented as represented in Figure 2; however, it can be sold in order to increase the revenues of the plant, as explained in Section 4.3.4.

Since alkaline electrolysis is an exothermic process working over thermoneutral voltage for a higher productivity, a cooling system is designed to remove the heat generated at nominal power with the purpose of maintaining the nominal operating conditions (Table S.2 in Supplementary Material).

Finally, the produced hydrogen was cooled and compressed (stream 107) to the operating conditions required at the inlet of the methanol synthesis section.

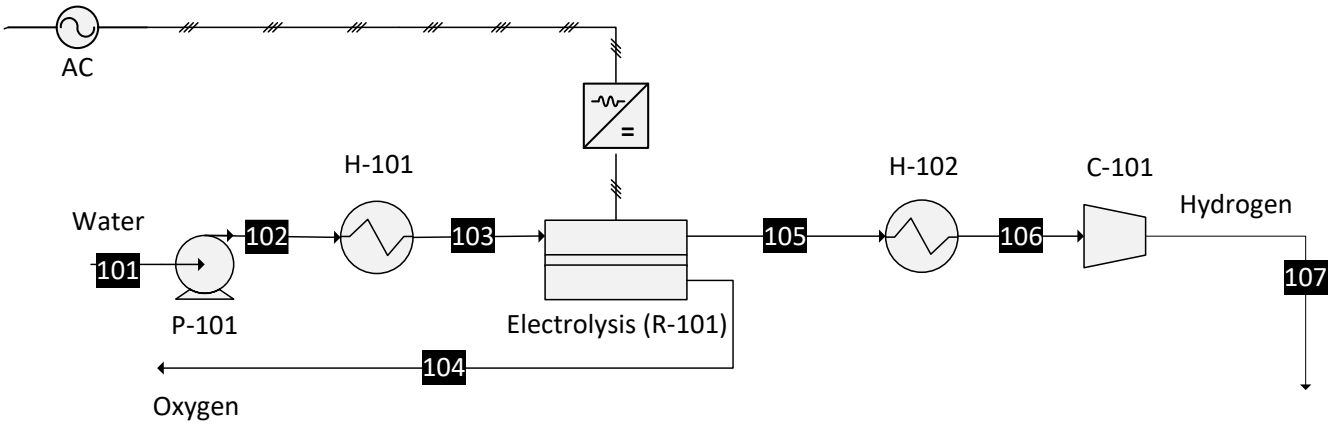

Figure 2 - Flowsheet of the model of water electrolysis section. Recirculation of excess feedwater is not shown

3.1.2.Carbon capture through amine scrubbing

The process of carbon capture from the exhaust gas of a coal-fired power plant through amine scrubbing was developed taking the cue from the real datasheet and operating results of the pilot plant described in Ref. [29]: Figure 3 shows the flowsheet of the model reporting the tags for the operating streams and the main blocks.

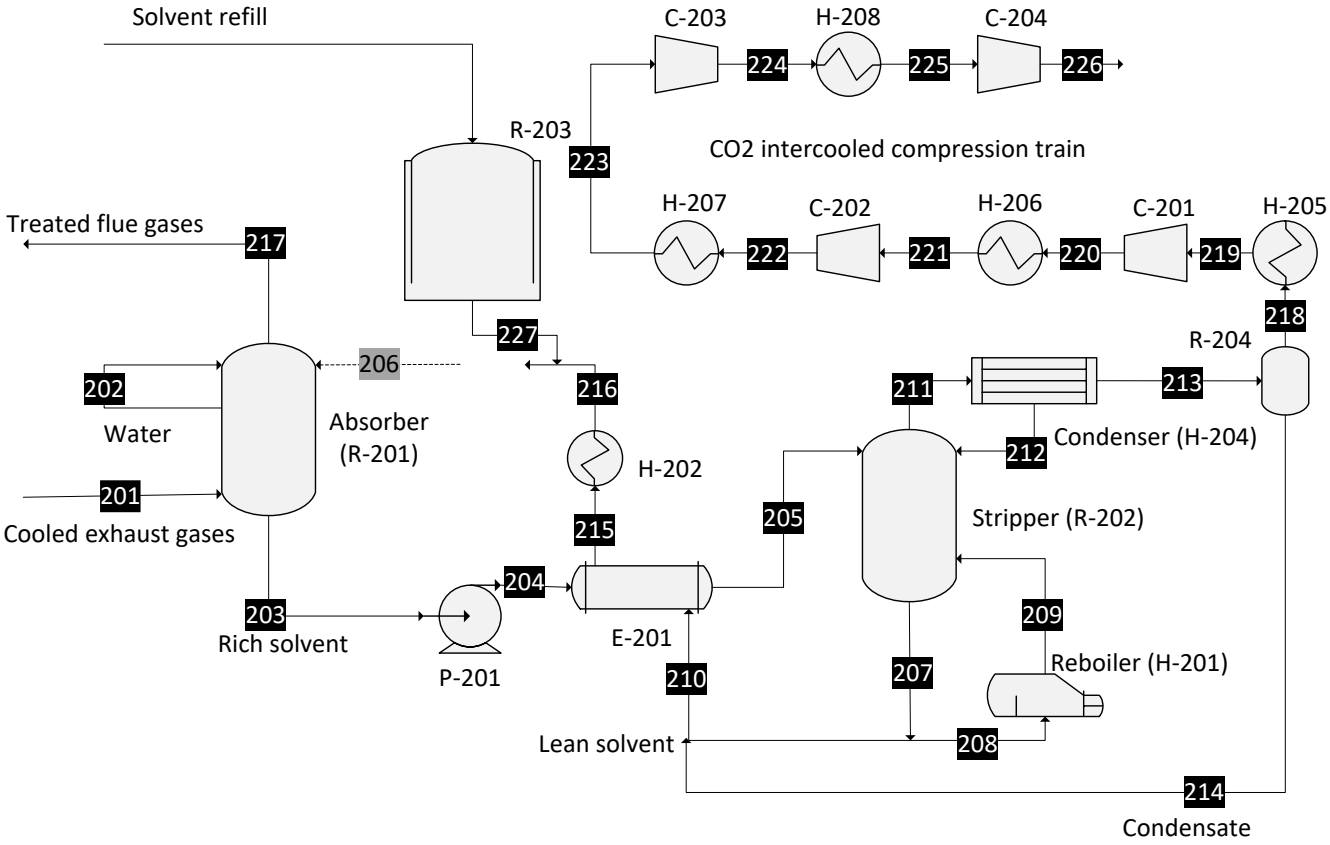

Figure 3 - Flowsheet of the model of carbon capture section

Table 3 lists the equilibrium and the kinetic-controlled reactions that describe the processes of chemical absorption and desorption of CO_2 [42].

Table 3 - Chemical reactions employed in the model of the carbon capture section

Reaction	Type	Reaction	Type
4) $H_2O + HCO_3^- \leftrightarrow CO_3^{2-} + H_3O^+$	Equilibrium	9) $OH^- + CO_2 \rightarrow HCO_3^-$	Kinetic
5) $2\ H_2O \leftrightarrow OH^- + H_3O^+$	Equilibrium	10) $HCO_3^- \rightarrow OH^- + CO_2$	Kinetic
6) $2\ H_2O + CO_2 \leftrightarrow HCO_3^- + H_3O^+$	Equilibrium	11) $MEA + CO_2 + H_2O \rightarrow MEACOO^- + H_3O^+$	Kinetic
7) $MEACOO^- + H_2O \leftrightarrow MEA + HCO_3^-$	Equilibrium	12) $MEACOO^- + H_3O^+ \rightarrow MEA + CO_2 + H_2O$	Kinetic
8) $MEAH^+ + H_2O \leftrightarrow MEA + H_3O^+$	Equilibrium		

The thermodynamic properties of the chemical species involved in the carbon capture process were estimated with the unsymmetrical electrolyte non-random two-liquid method for the liquid phase, Redlich-Kwong equation and Henry's Law for gas phase. In two-phase blocks like the ab-/desorption columns, the mass transfer was modelled with a "two-film" rate-based approach neglecting the mixing by convection [43,44].

The developed model was tuned in order to follow the specifications and the results reported by Notz et al. [29]. It is worth remarking that the carbon capture loop was modelled as an open system in order to avoid convergence issues with Aspen Plus™: the lean solvent regenerated in the stripper (stream 216) is not fed directly to the absorption column. Instead, we employed a fictitious feed of lean solvent (stream 206) characterized by the same loading α reported in the consulted experimental results [29]:

$$\alpha = \frac{moles\ of\ CO_2\ species}{moles\ of\ MEA\ species} = 30.8\% \qquad \text{(Eq. 1)}$$

The non-zero loading of the solvent fed to the absorber accounts for the fact that the solvent cannot be completely regenerated in a real closed-loop continuous operation (i.e. a part of CO_2 keeps being dissolved in or chemically bound to the solvent) unless a high amount of heat is consumed in the reboiler of the stripper. To ensure the mass balance of the lean solvent, we introduced a design specification that determines the regeneration heat duty in the stripper reboiler (H-201) needed to guarantee that the loading of stream 216 equals the loading of stream 206.

The mass streams and the energy fluxes of the developed model were compared with those of the reference pilot plant and the model was validated considering the following operating parameters:

$$CO_2\ \text{removal rate},\ \Psi = \frac{\dot{m}_{218\,(CO2)}}{\dot{m}_{201\,(CO2)}} \qquad \text{(Eq. 2)}$$

$$\text{Specific regeneration heat duty, } q_{reb} = \frac{\dot{Q}_{H-201}}{\dot{m}_{218\,(CO2)}} \quad \text{(Eq. 3)}$$

$$\text{Liquid solvent to flue gas ratio in the absorber, } \frac{L}{G} = \frac{\dot{m}_{206}}{\dot{m}_{201}} \quad \text{(Eq. 4)}$$

Where $\dot{m}_{218\,(CO2)}$ and $\dot{m}_{201\,(CO2)}$ (kg/s) are the mass flow rates of CO_2 in streams 218 and 201, respectively; $\dot{Q}_{H-201}$ (kW) is the regeneration heat duty consumed by the stripper reboiler; $\dot{m}_{206}$ and $\dot{m}_{201}$ are the mass flow rates of streams 206 and 201, respectively. The following table reports the results of the validation of the developed model.

Table 4 - Validation of the developed model

Operating parameter	Results of the pilot plant [29]	Developed model	Deviation
CO_2 removal rate, Ψ	51.3%	51.7%	0.78%
Specific regeneration heat duty, q_{reb} (kJ/g$_{CO2}$)	4.68	4.64	0.85%
L/G ratio	2.76	2.76	-

The validated model was then scaled up to the industrial size of the studied Power-to-MeOH system, keeping the operating conditions, the design specifications and the configurations of each component unchanged, apart the size of the absorption and desorption columns (Table S.4 in Supplementary Material). The typical value of Ψ used for the analysis of modelled carbon capture process [45–47] and the design of real amine scrubbing plants [48,49] is 90%, which is higher than the value from the reference plant used in the validated model (51.7%). Hence, we adopted a CO_2 removal rate of 75% for the scaled-up model of the carbon capture section as a trade-off between the mentioned data, also considering that Notz et al. [29] report another experiment at lower CO_2 partial pressure resulting with Ψ= 75%. From this point on, the analysis refers uniquely to the validated scaled-up model.

Table S.3 in the Supplementary Material reports the values of the chemical and physical properties of the streams entering the carbon capture section, i.e. flue gas mixture coming from the upstream power plant (stream 201 in Figure 3), the fresh solvent refilled in the ab-/desorption loop in order to compensate the leakages due to entrainment and evaporation (stream 226 in Figure 3) and the fictitious lean solvent stream 206.

Table S.4 in Supplementary Material lists the detailed specifications of the two ab-/desorption columns: these blocks were simulated as rate-based multi-stage vapor-liquid fractionating unit (RadFrac components in Aspen Plus™) with two-film approximation.

3.1.3.Methanol synthesis

In this section, the captured carbon dioxide is hydrogenated and converted into methanol. In order to simulate this process, the model developed by Calogero [30] and based on the work by Atsonios et al. [25] was used as reference. The model was rescaled to fit the flow rate of CO_2 captured in our case study and integrated in our model.

As shown in Figure 4, the feeding stream 301 (characterized by an H_2/CO_2 ratio equal to 3), was mixed with the recirculated excess reactants (stream 311). In order to guarantee the operating conditions of T=250°C and p=65 bar (see Table S.5 in Supplementary Material), the feeding mixture is preheated before entering the reactor (recovery heat exchanger E-301 and heater H-301).

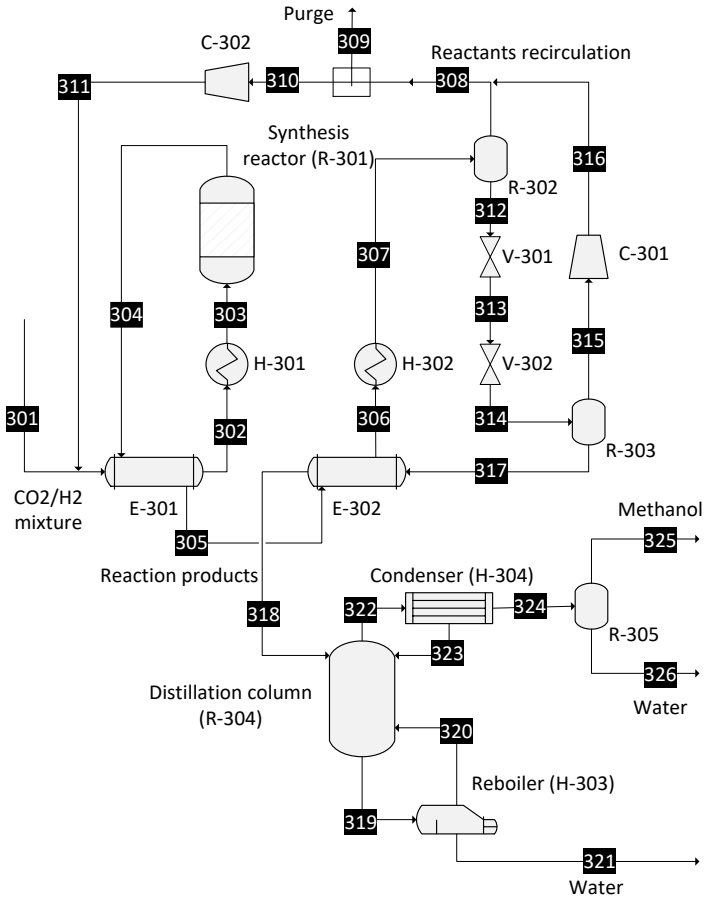

Figure 4 - Flowsheet of the model of methanol synthesis section

The reactor for methanol synthesis (see Table S.6 in Supplementary Material for the specifications) was modelled as a horizontal isothermal plug-flow reactor with the kinetic scheme proposed by Calogero [30]. The $Cu/ZnO/Al_2O_3$ solid catalyst in the reactor enhanced the hydrogenation of CO_2, producing methanol according to the reactions reported in Table 5 proposed by Graaf's kinetic model [50].

Table 5- Chemical reactions employed in the model of the methanol synthesis section

Reaction	**Enthalpy Variation**
13) $CO_2 + 3\ H_2 \leftrightarrow CH_3OH + H_2O$	$\Delta H_{25°C} = -49.5\ kJ/mol_{CO2}$
14) $CO_2 + H_2 \leftrightarrow CO + H_2O$	$\Delta H_{25°C} = +41.2\ kJ/mol_{CO2}$
15) $CO + 2\ H_2 \leftrightarrow CH_3OH$	$\Delta H_{25°C} = -90.7\ kJ/mol_{CO2}$

After the reactions, the pressure and the temperature of the fluid were decreased through two throttling valves and a recovery heat exchanger in order to reach the thermodynamic conditions required in the distillation column (T=85°C, p=2.2 bar). The distillation column was modeled considering 60 stages with reboiler pressure of 1.1 bar and a pressure drop of 0.1 bar along the column height. A mechanical demister was added to separate water from the distillate in order to obtain methanol with a degree of purity of 99.9% (stream 325).

3.2. Thermal integration

The demand of external energy in terms of heating ($\dot{Q}_{heating}$) and cooling needs ($\dot{Q}_{cooling}$) of the whole Power-to-MeOH was minimized exploiting the endothermicity and exothermicity of the different components. To this end, the pinch analysis methodology was applied to identify the hot and cold fluids (Figure 5) and to design a network of recovery heat exchangers for an improved energy integration of the plant. An arbitrary minimum temperature difference (ΔT_{min}) of 10 °C was assumed for the coherent coupling of different streams, while an average specific heat capacity (c_p, kJ/kg/K) was set in the range between inlet and outlet temperatures of each stream.

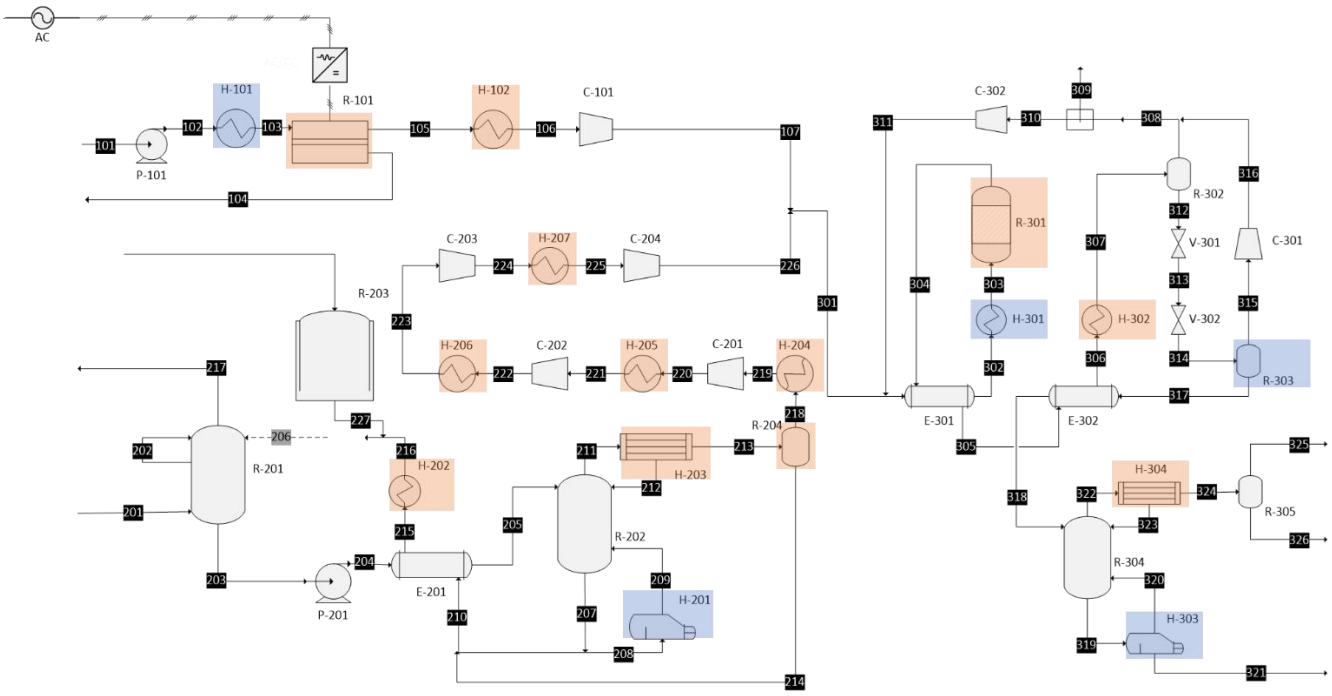

Figure 5 - Identification of the hot fluids (red boxes) and cold fluids (blue boxes) involved in the pinch analysis

3.3. Techno-economic assessment

The results of the steady-state models of the three sections and their thermal integration were used as input data for the assessment of the techno-economic feasibility of the Power-to-MeOH system through the revenue accounting methodology. The boundaries of the techno-economic assessment include the components represented in the colored boxes in Figure 1 and the streams and energy fluxes entering and leaving the whole system. For the analysis, we introduced three different techno-economic scenarios in order to provide a -15%/+30% confidence range in which the values of the TOC and the main economic indicators are expected to be:

- Scenario 1 – optimistic, with economic assumptions to define the lower value of the TOC;
- Scenario 2 – realistic, relying on data from pilot plant projects, in literature and from reports of R&D organizations [51–54].
- Scenario 3 – pessimistic, corresponding to the upper bound of the confidence range for TOC.

In all the scenarios, we assumed a project lifetime of 25 years and 8000 operating hours per year.

3.3.1. CAPEX estimation: scenarios and assumptions

A bottom-up approach was adopted for the definition of the TOC, employing the sizes (*S*) of the different components in the plant as input variables of cost functions available in literature. For each of the main components present in the studied system (packed columns, reactors, tanks, heat exchangers, pumps, compressors and flash separators), the cost functions from Turton et al. [52] were employed to evaluate the purchased cost C_p^0 assuming carbon steel as construction material and operating pressure of 1 bar:

$$\log_{10} C_p^0 = K_1 + K_2 \log_{10} S + K_3 [\log_{10} S]^2 \quad \text{(Eq. 5)}$$

The parameters K_1-K_3 and the range of sizes [S_{min}, S_{max}] of validity of the cost functions were also provided in Ref. [52]. If the size *S* of the component was out of the [S_{min}, S_{max}] range, we applied the following approximation with the cost exponent *n* equal to 0.6 (six-tenths rule) in lack of further indications [55]:

$$C_p^0 = \begin{cases} C_p^0(S_{min}) \cdot \left(\frac{S}{S_{min}}\right)^n, & S < S_{min} \\ C_p^0(S_{max}) \cdot \left(\frac{S}{S_{max}}\right)^n, & S > S_{max} \end{cases} \quad \text{(Eq. 6)}$$

In order to estimate the bare module cost of the effective component, one should introduce the factor F_M accounting for the real construction material and the factor F_P accounting for changes in operating pressure:

$$C_{BM} = C_p^0 \cdot F_{BM} = C_p^0 \cdot \left(B_1 + B_2 F_p F_M\right) \quad \text{(Eq. 7)}$$

Turton et al. [52] report the factor F_M according to the considered construction material and the constants B_1 and B_2 for heat exchangers, vertical/horizontal process vessels and pumps; for the remaining components, the bare module factor F_{BM} is provided. The cost functions provided by Turton et al. refer to the year 2001; we updated the bare module costs to year 2019 using the ratio of CEPCI (Chemical Engineering Plant Cost Index, [56]) values to account for the effect of inflation:

$$C_{BM}(2019) = C_{BM}(2001) \cdot \frac{CEPCI_{2019}}{CEPCI_{2001}} = C_{BM}(2001) \cdot \frac{618{,}7}{394} \quad \text{(Eq. 8)}$$

The first value of the \$/€ exchange rate in 2019 (1 € = 1.145 \$) was used for conversion from US dollars (the reference currency used in [52]) to Euros.

Once determined $C_{BM,main}$ as the sum of all the bare module costs of the main components, the Bare Erected Cost (BEC) of the plant is estimated considering the cost of minor equipment and machinery and the supporting work. These items are estimated as a fraction of $C_{BM,main}$, as explained in the following table:

Table 6 - Scenarios and assumptions for the estimation of the BEC of the plant [52]

	Sc.1 - optimistic	Sc.2 - realistic	Sc.3 - pessimistic
$C_{BM,main}$	71.2%	68%	63.1%
Pipe, valves and fittings	18.0%	20.0%	23.0%
Process instruments & control	6.3%	7.0%	8.1%
Electric equipment and materials	4.5%	5.0%	5.8%
$C_{BM,tot}$	100%	100%	100%
$C_{BM,tot}$	71.2%	68%	63.2%
Erection and installation labor	21.6%	24%	27.6%
Buildings, materials and labor	7.2%	8%	9.2%
BEC	100%	100%	100%

Concerning the electrolysis system, the following cost function valid for the total cost of alkaline electrolyzers with size bigger than 2 MW (including the stack, power converters, water purification system, gas purification unit and water recirculation pump) was derived fitting the data reported in [57]:

$$\tilde{c}_{BM,WE} = 1437 \cdot {P_{WE}}^{-0.095} \quad \text{(Eq. 9)}$$

where $\tilde{c}_{BM,WE}$ is the total specific cost of the electrolysis module (€/kW) and P_{WE} is the nominal stack size (kW). We obtained a specific cost of 599 €/kW for a 10-MW electrolyzer (i.e., the total bare module cost $C_{BM,WE}$ is 5.99 M€).

We followed the guidelines reported by NETL [51] for the estimation of the TOC, with the assumptions listed in Table 7. Process contingencies compensate for performance uncertainties and are applied as a fraction of BEC to each section of the plant according to the level of maturity of the technology.

Table 7 - Scenarios and assumptions for the estimation of the TOC [51]

	Sc.1 - optimistic	Sc.2 - realistic	Sc.3 - pessimistic
EPC contractor services (%BEC)	15.0%	17.5%	20.0%
Process contingencies PC (%BEC)	*	*	*
Project contingencies (%(EPCC+PC))	15.0%	15.0% [54]	30.0%
Start-up cost (%TPC)	1.8%	2.0%	2.3%
Inventory (%TPC)	0.45%	0.50%	0.58%
Financing costs (%TPC)	2.4%	2.7%	3.1%
Other owner's costs (%TPC)	13.5%	15.0%	17.3%

* PC: 0% – 5% – 10% for water electrolysis section;

5% – 17.6% [53] – 20% for carbon capture section;

0% – 5% – 10% for methanol synthesis section.

3.3.2. OPEX estimation: scenarios and assumptions

For the techno-economic assessment we also considered the following operating costs (OPEX) of the system, with $OC_{1\text{-}7}$ being variable operating costs proportional to the productivity of the Power-to-MeOH system and $OC_{8\text{-}9}$ being fixed costs not dependent on the flows of energy and/or mass consumed by the plant:

- OC_1. Electric energy consumed for the self-consumption of the Balance of Plant (compressors, pumps, etc.) and to feed water electrolysis.
- OC_2. Water supply for the different processes (water electrolysis, solvent makeup in carbon capture section), with a unit cost of 3.36 €/m^3.
- OC_3. Tap water (c_p = 4.186 kJ/kg/K) operating between 12 °C and 15 °C used to cool down streams that are at temperature higher than or equal to 25 °C, with a unit cost of 3.36 €/m^3.
- OC_4. Hot utility to fulfil the thermal energy demand of the system through electric heaters with a power-to-heat efficiency of 95%.
- OC_5. Refill of MEA in carbon capture section due to loss of solvent, with a unit cost of 1.09 €/kg [47].
- OC_6. Replacement of the electrolysis stack at 11th and 21st year of operation with the following cost [58]:

$$OC_6 = \frac{2 \cdot C_{BM,WE} \cdot 0.4}{3} \quad \text{(Eq. 10)}$$

- OC_7. Replacement of the Cu/ZnO/Al_2O_3 catalyst in the methanol synthesis reactor, with a unit cost of 95.24 €/kg [28].
- OC_8. Maintenance, assumed as 3% of Total Plant Cost (TPC) [47].

- OC_9. Insurance, assumed as 1% of Total Plant Cost (TPC) [47].

Labor costs were excluded from the analysis since they strongly depend on the plant location. All the OPEX items are assumed to be constant during the plant lifetime. Concerning OC_1 and OC_4, we considered different options to fulfil the electric demand of the whole system with RES. The following table reports the levelized cost of electricity (LCOE) for each of the considered renewable sources in 2018 [59], considering a $/€ exchange rate of 1.145:

Table 8 - Global electricity costs from RES in 2018 [59]

Renewable source	**Scenario**	**Global weighted-average cost of electricity (€/MWh, 2018)**	**Cost of electricity: 5th and 95th percentiles (€/MWh, 2018)**
Bioenergy	A	54.15	41.92 – 212.23
Geothermal	B	62.88	52.4 – 124.89
Hydro	C	41.05	26.2 – 118.78
Solar PV	D	74.24	50.66 – 191.27
Conc. solar power	E	161.57	95.2 – 237.55
Offshore wind	F	110.92	89.08 – 172.93
Onshore wind	G	48.91	38.43 – 87.34

As explained in Section 3.4, we did not consider the sale of methanol at a market price in the cash flow analysis, rather we computed its production cost (COM, cost of methanol) that allows to reach a breakeven at the end of plant lifespan. Apart from methanol, the only other stream of the Power-to-MeOH system (shown in Figure 1) with an interesting market value is oxygen. We will discuss (Section 4.3.4) the sensitivity of the economic figures of merit (Section 3.4) to the sale of oxygen, considering a range for its market price:

- 0 €/t (i.e., oxygen is vented);
- 70 €/t [60,61] associated to liquefied oxygen;
- 150 €/t [62] associated to oxygen compressed at 30 bar.

3.3.3. Cash flow analysis and revenue accounting methodology

The economic feasibility of the investment project was verified with the cash flow analysis methodology, with the assumptions of no discount nor escalation rate when estimating the annual cash flows during the plant lifetime and of no remuneration of the invested capital. The following equations were used, where *k* represents the time passed since the investment (year 0):

- Earnings before interest, taxes, depreciation and amortization:

$$EBITDA_k = \sum_i R_i - \left| \sum_j OC_j \right| \quad \text{(Eq. 11)}$$

with OC_j referring to the operating costs listed in Section 3.3.2 and R_i to the revenue from sale of methanol and oxygen (if considered, as already anticipated in Section 3.3.2 and thoroughly discussed in Section 4.3.4).

- Amortization of the invested capital:

$$A_k = \frac{|TOC|}{n_{life}} \quad \text{(Eq. 12)}$$

where n_{life} is the plant lifetime (25 years)

- Earnings before interest and taxes:

$$EBIT_k = EBITDA_k - |A_k| \quad \text{(Eq. 13)}$$

- Taxes:

$$Tax_k = \%_T \cdot EBIT = 24\% \, EBIT \quad if \; EBIT > 0 \quad \text{(Eq. 14)}$$

where 24% is the corporate income tax rate in law in Italy since 2017.

- Free Cash Flow:

$$FCF_k = EBITDA_k - |Tax_k| \quad \text{(Eq. 15)}$$

- Total Investment Cost, i.e. the total flow of money expended (costs) during the plant lifetime:

$$TIC = -|TOC| - \sum_{k=1}^{n_{life}} \left| \sum_j OC_{j,k} \right| \quad \text{(Eq. 16)}$$

3.4. Key Performance Indicators of the system

The performance of the system was assessed from both technical and economic standpoints, with particular attention to the reduction of the impacts with respect to the zero-alternative.

- The main environmental benefit of the studied system consists of the reduction of carbon emissions to the atmosphere: m_{CO2} indicates the mass (t/y) of carbon dioxide captured and converted to methanol on annual basis.
- Water consumption represents an important issue for the sustainability of the process: hence, we also assessed the annual amount (m^3/y) of tap water V_{H2O} consumed in the different sections.
- Specific plant energy consumption for CO_2 avoided (SPECCA, kWh/kg_{CO2}), i.e., the total consumption of electric energy and heat (assuming that they have the same exergy level) of carbon capture section to remove a unit of CO_2 from the flue gas stream and convey it to the methanol synthesis section:

$$\text{SPECCA} = \frac{E_{\text{el}_{CO2}} + Q_{th_{CO2}}}{m_{CO2}} \quad \text{(Eq. 17)}$$

- The global efficiency of the Power-to-MeOH plant, considering the electric ($E_{\text{el}_{sys}}$) and thermal consumption ($Q_{th_{sys}}$) of the whole system to produce the annual amount of MeOH (m_{MeOH}), characterized by the lower heating value LHV_{MeOH} reported in Table 1:

$$\eta_{\text{gl}} = \frac{m_{MeOH} \cdot \text{LHV}_{MeOH}}{E_{\text{el}_{sys}} + Q_{th_{sys}}} \quad \text{(Eq. 18)}$$

- As main indicator of the techno-economic feasibility of the system, we assessed the cost of methanol (COM, €/kg_{MeOH})

$$COM = \frac{-TIC - |R_{O_2}|}{m_{MeOH} \cdot n_{life}} \quad \text{(Eq. 19)}$$

as the production cost of methanol that ensures a breakeven over the project lifetime of 25 years. We compared it with the current and forecasted market prices of methanol. COM was assessed in the three different scenarios for the definition of the TOC (Section 3.3) and considering the three options for oxygen sale (R_{O2}) presented in Section 3.3.2 (selling price: 0-70-150 €/t). In the most and in the least competitive configurations, we also estimated the values of levelized cost of methanol (LCOM) ensuring an internal rate of return (IRR) of the investment ranging from 0 to 10%:

$$IRR = i: \sum_{k=1}^{n_{life}} \frac{FCF_k}{(1+i)^k} - |TOC| = NPV = 0 \quad \text{(Eq. 20)}$$

Since the discount rate strongly depends on investment structure and market conditions and affects the cash flow analysis, we preferred not to assess NPV (net present value), rather to provide the LCOM associated to the parameterized values of the discount rate (i.e., IRR) that ensures a breakeven at the end of plant lifetime – or, in other words, NPV = 0.

- As an additional indicator, we provided the Payback Period (PBP), i.e., the number of years it takes to break even from the investment considering the annual net free cash flows:

$$PBP = min\left\{ k \;\middle|\; -|TOC| + \sum_{k=1}^{n_{life}} FCF_k > 0 \right\} \quad \text{(Eq. 21)}$$

4. Results and discussion

We modelled the full Power-to-MeOH chain with the capture of about 1.25 t/h of carbon dioxide in 10.2 t/h of exhausts from a coal-fired power plant and its further conversion to 788 kg/h of methanol through a catalytically driven thermochemical reaction with 1.9 kNm^3/h of electrolytic hydrogen. The outcomes of these simulations are presented in this section, along with the results of thermal integration, energy analysis and economic assessment.

4.1. Steady-state simulation of the plant

This section reports the energy balance resulting from the simulations and the results obtained from the thermal integration calculations.

4.1.1.Energy balance

Table 9 summarizes the energy balance of the full Power-to-MeOH chain, reporting the exchanges of power and heat in the different sections of the plant to produce 788 kg/h of methanol (i.e. about 4.36 MW of chemical power, considering the chemical data in Table 1). Considering the most representative streams of water electrolysis, carbon capture and methanol synthesis sections, the relevant information about mass balance and the thermodynamic conditions of each streams resulting from the simulations are reported in Table S.7 in the Supplementary Material. The IDs refer to Figure 5.

The left-hand side of Table 9 reports the heat fluxes exchanged between the plant components and the environment (negative values refer to the cooling duties). The main thermal fluxes exceeding 1 MW derive from the cooling of excess feedwater recirculation in the electrolyzer, the carbon capture solvent heating for CO_2 stripping, the preheating of the H_2/CO_2 reactant mixture entering the methanol synthesis reactor and the cooling of products mixture at the inlet of distillation column. The presence of many heat fluxes with opposite signs justifies the investigation about thermal integration of the different sections to reduce cooling and heating demands of the plant.

Concerning electric energy consumption on the right-hand side of the table, power demanded to run electrolysis is 2-3 orders of magnitude higher than other contributions listed, which sum up to about 392 kW. In order to certify the produced methanol as "green", the power demand should be fulfilled by a sufficiently high renewable generation (scenarios A-G in Table 8), hence excluding any indirect emission of CO_2. We accounted for this renewable energy consumption in the energy balance and the KPIs, without modelling its daily/seasonal fluctuations. A first rough estimation of 42.48% for the power-to-MeOH process gross efficiency is computed considering the power demanded to run electrolysis as the only energy consumed by the plant and converted into the chemical power of 788 kg/h of methanol. This figure of merit will be compared with the values of the global plant efficiency (Section 4.2) accounting also for the thermal needs.

Table 9 – Energy balance of the Power-to-MeOH system

ID	Component Description	Heat duty (kW)
H-101	Electrolysis water preheating	116.28
R-101	Rec. excess water cooling	-3482
H-102	Hydrogen cooling	-37.48
E-201	Solvent recovery heat exchanger	±1804.7
H-201	Reboiler of the stripper	1268.52
H-202	Lean solvent cooling	-502.4
H-203	Condenser of the stripper	-150.14
H-204	CO_2 intercooling stage #1	-18.36
H-205	CO_2 intercooling stage #2	-26.75
H-206	CO_2 intercooling stage #3	-26.66
H-207	CO_2 intercooling stage #4	-25.68
E-301	Recovery heat exchanger	±909.94
E-302	Recovery heat exchanger	±125.14
H-301	Reactants preheating	1030.53
R-303	Flash sep. of MeOH mixture	77.36
H-302	Cooling of products mixture	-1820.4
H-303	Reboiler of the distill. column	313.19
R-301	MeOH synthesis heat of reaction	-426.05
H-304	Condenser of the distill. column	-426.11

ID	Component description	Electric power (kW)
P-101	Electrolysis feedwater pumping	0,56
R-101	Electrolysis module	10260
C-101	Hydrogen compression	194.92
P-201	Rich solvent pumping	2.76
C-201	CO_2 post-compression	25.85
C-202	CO_2 post-compression	25.52
C-203	CO_2 post-compression	25.06
C-204	CO_2 post-compression	24.68
C-301	Compression of the rec. reactants	92.71
C-302	Compression of the rec. reactants	≈ 0

ID	Component description	Chemical content (kW)
326	Methanol production	4358.2

4.1.2.Results of pinch analysis

As reported earlier, the fulfilment of thermal energy demands for the conditioning of the streams operating in the plant heavily affects the system feasibility. The presence of different fluids heating and cooling in the sections offers the opportunity of reducing the thermal demand of the plant. Hence, we applied pinch analysis methodology to minimize the heat supplied from external thermal sources through a network of recovery heat exchangers.

Setting an arbitrary minimum temperature difference (ΔT_{min}) of 10 °C, the pinch point (T_{pp}) of the plant was found at 108.5°C. Table 10 reports the sensible reduction of both cooling (-47%) and heating (-81%) demand after the thermal integration of the different sections of the plant, with a beneficial effect on the energy performance of the process. Of the 5193 kW of cooling duty after integration, about 4767 kW are associated to streams cooling down at temperatures higher than 25°C: this cooling duty will be fulfilled using tap water undergoing an increase in temperature equal to 3°C. The remaining 8% of cooling demand corresponds to the duty of the condenser in the distillation column operating at around -18°C: considering its limited weight on the global energy demand, this contribution is neglected in the techno-economic assessment and the evaluation of the KPIs of the plant. The heating demand resulting after thermal integration (1057.3 kW) is almost totally associated to the preheating of H_2/CO_2 reactant mixture (cf. 1030.53 kW in Table 9) from 151°C to the operating temperature of the methanol synthesis reactor, 250°C.

Table 10 – Reduction of heat demand thanks to thermal integration

	$\dot{Q}_{heating}$ [kW]	$\dot{Q}_{cooling}$[kW]
W/out Thermal Integration	5645.72	9781.79
With Thermal Integration	1057.30	5193.38

The above-mentioned results are reported using hot and cold composite curves in Figure 6, which highlights the recovery of about 4588 kW corresponding to the range in which the two curves overlap: a design of the network of recovery heat exchangers for the improved energy integration of the plant is reported in Figure S.1 in the Supplementary Material.

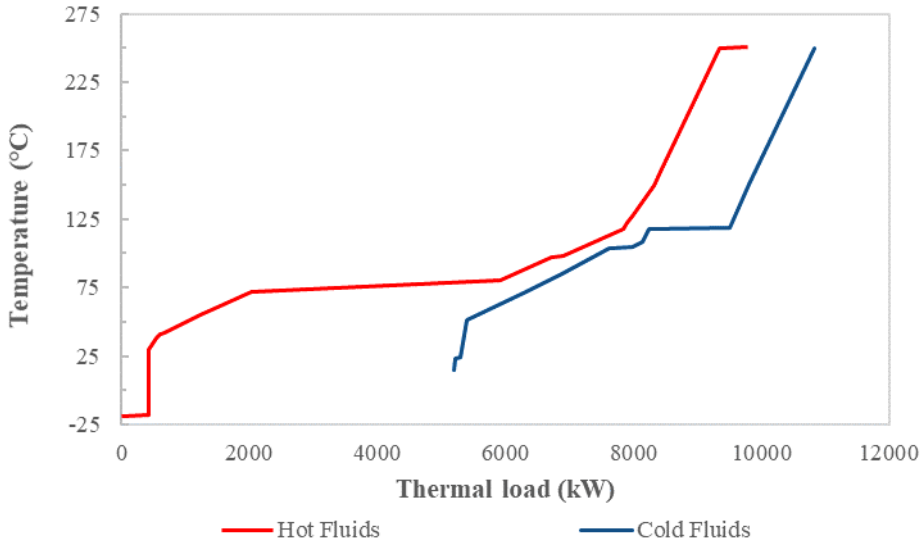

Figure 6 - Hot and cold composite curves resulting from pinch analysis

4.2. Energy and environmental performance

Table 11 reports the values of the KPIs defined in Section 3.4 to assess the performance of the Power-to-MeOH system from energy and environmental standpoints. The capture of a constant flow of about 1.25 t/h of CO_2 from the coal-fired plant exhausts and the exploitation of renewable energy to run the plant ensure an annual emission reduction to the atmosphere of 9968 tons of CO_2.

The annual water consumption resulting from the simulations run is about 12,635 m^3, of which:

- 1005 m^3 (ca. 8%) to refill water in the carbon capture solvent due to evaporation and entrainment;
- 8593 m^3 (ca. 68%) to feed electrolysis;
- 3037 m^3 (ca. 34%) as fluid fulfilling the cooling demand of the plant.

The estimation of the different shares highlights that water electrolysis is the most consuming section not only for what concerns electric energy, but also water. Following a Power-to-MeOH scheme through the electrochemical conversion of renewable energy into hydrogen, this issue is unavoidable and must be carefully accounted for when assessing the plant location and the consequent impacts on water availability in different socio-economic contexts.

The benefits of the thermal and mass integration become evident also when analyzing the SPECCA. The specific energy consumption of carbon capture section without thermal integration (i.e. considering power consumption and heating demand associated to the components of carbon capture section in Table 9) is around 1.25 kWh/kg_{CO2}. This value is in line with the typical values of traditional post-combustion applications in coal-fired power plant,

0.72-1.53 kWh/kg_{CO2} [33] for the regeneration of a commercial 7m MEA solvent. The integration of the sections reduced the thermal demand of the full Power-to-MeOH chain, avoiding the need of an external heat source for carbon capture section thanks to the network of recovery heat exchangers, but limiting thermal supply to the heater at the inlet of methanol synthesis reactor (H-301). In this way, $Q_{th_{CO_2}}$ in (Eq. 17), accounting mainly for the regeneration heat duty at the stripper reboiler, becomes 0 and the SPECCA drastically reduces to 0.094 kWh/kg_{CO2}.

The global efficiency of the plant accounts for the transformations occurring in all the sections of the Power-to-MeOH conversion process. The reduction from the 42.48% gross efficiency reported earlier to 37.22% (Table 11) is mostly due to the residual heating demand after thermal integration, with a smaller influence of power consumption of compressors and pumps. It is worth remarking that η_{gl} would be equal to 26.74% in lack of thermal integration: the 81% reduction of heating demand thanks to thermal integration allows a strong improvement of the system performance.

Table 11 – Key Performance Indicators

Key Performance Indicator	Unit	Value
Reduction of carbon emissions to the atmosphere, m_{CO2}	t/y	9968
Water consumption, V_{H2O}	m^3/y	$12.63*10^3$
SPECCA (w/out thermal integration)	kWh/kg_{CO2}	1.248
SPECCA (with thermal integration)	kWh/kg_{CO2}	0.094
Global efficiency of the Power-to-MeOH plant, η_{gl}	-	37.22%

4.3. Results of the techno-economic assessment

Starting from the results of the simulation of the steady-state operation of the plant, we carried out a techno-economic analysis following a bottom-up approach for the determination of the Total Overnight Cost under three different techno-economic scenarios (1-optimistic, 2-realistic, 3-pessimistic) and the operating costs considering different RES to fulfil the plant electricity demand. The following sections report these results and the main indicators of plant economic viability identified in Section 3.4: COM (cost of methanol) and IRR (Internal Rate of Return) with its levelized cost of methanol (LCOM), investigating the possibility of selling electrolytic oxygen.

4.3.1.Estimation of the Total Overnight Cost

The size of each component was determined according to the results of the simulations run with Aspen Plus™ at the nominal operating point of the plant. Following the bottom-up procedure described in Section 3.3.1, we estimated the bare module cost of each of the major components in the plant (represented in the scheme in Figure 1) and we defined a confidence range of the TOC of the plant introducing the three economic scenarios. The TOC of the 788-kg/h power-to-MeOH plant is between 27.7 M€ (scenario 1-optimistic) and 40.2 M€ (scenario 3-pessimistic), with a realistic estimate of 31.1 M€, of which we can allocate:

- 6% to carbon capture section;
- 43-45% to water electrolysis section;
- 5-6% to methanol synthesis section;
- 43-45% to the TOC of the network of recovery heat exchangers (including heaters and coolers) resulting from the pinch analysis and designed in Figure S.1 in the Supplementary Material.

Although increasing the initial investment cost, the realization of the heat recovery network allows to reduce the operating costs for the correct thermal management of the plant, exploiting the available resources in a smarter way. The fulfilment of heating and cooling demands with external heat sinks and sources would increase the OPEX.

The cost of a scheme without any thermal integration (like in Figure 1) would probably be lower and allocated in the different sections. Also, in this case, the main part of the plant TOC would be allocated to the water electrolysis section due to the high specific cost of the electrolyzer. Even though alkaline stacks are the most mature technology for water electrolysis, the volumes installed worldwide for stationary conversion and/or storage applications are still limited. Incentives for the commercial use of electrolytic hydrogen as a vector for the long-term storage of RES would be of vital help for a rapid cost decrease, hence making systems like the examined Power-to-MeOH plant more economically viable.

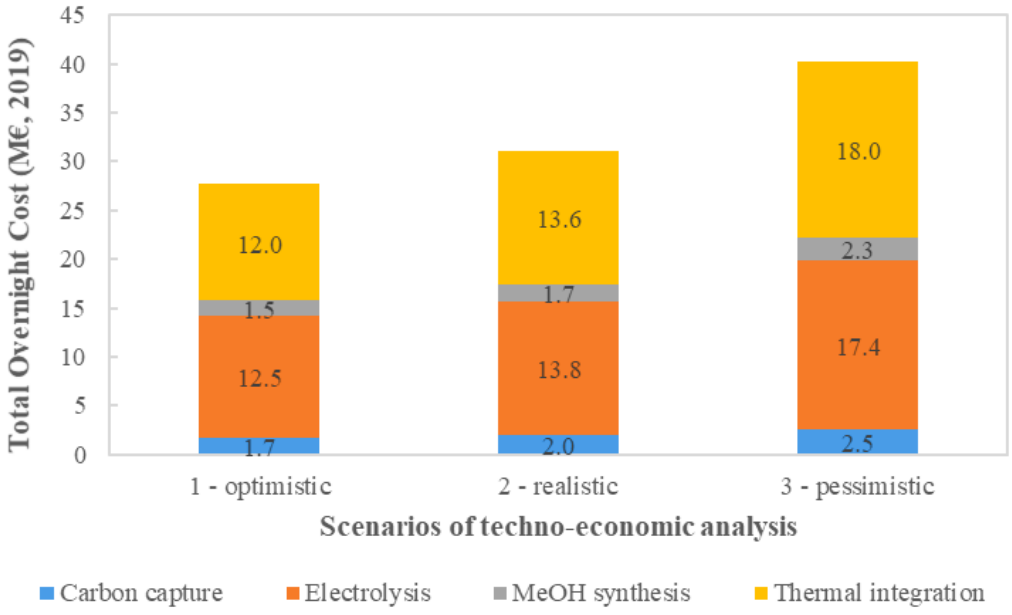

Figure 7 - Contribution of each section to the CAPEX in the different techno-economic scenarios

4.3.2.Estimation of the Operating Costs

The Operating Costs (OPEX) of the whole plant contributing to the definition of the Total Investment Cost (TIC, Eq. 16) in the cash flow analysis were divided in fixed and variable costs. In particular, the fixed costs include the maintenance and the insurance costs; variable costs include costs $OC_{1\text{-}7}$ reported in the lists in Section 3.3.2. The estimation of the maintenance and the insurance costs as percentage of the Total Plant Cost (TPC) justifies the variation of the fixed OPEX in the three techno-economic scenarios, as reported in Table 12. The item "Variable OPEX" in the same table includes:

- 32.7 k€/year for water supply to the different processes (OC_2);
- 10.2 k€/year for cooling water (OC_3);
- 4.8 k€/year for MEA refill (OC_5);
- 130.8 k€/year for the electrolysis stack replacement (OC_6, supposing to amortize the expenses at 11th and 21st year over the whole plant lifetime of 25 years);
- 3 k€/year for the replacement of the methanol synthesis catalyst (OC_7).

The last operating costs OC_1 and OC_4 are associated to the consumption of electric energy. As explained earlier, we investigated different scenarios in which the required power supply comes from different renewable energy

sources (cases A-G listed in Table 8), each with its average cost. Hence, the cost of feeding the 94.13 GWh/year to run the plant ranges from a minimum value of 3.86 M€/year of hydropower (case C) to a maximum value of 15.2 M€/year in case of CSP (concentrated solar power, case E). This range reflects the different levels of technology readiness, maturity and availability of the two solutions. In any case, feeding the power demand of the plant represents the main operating cost: thus, the choice of the source to produce renewable energy has a strong impact of the economic viability. The cheapest of the new-generation RES is onshore wind (case G): its cost is just 19% higher than hydropower. While hydropower can be installed only in locations with suitable water basins and watercourses ensuring a certain level of availability, wind is a resource that is more distributed worldwide. However, a suitable hydrogen buffer charging and discharging continuously would be required to face the power demand-generation mismatch and the unpredictable variations of wind, hence with an effect on the costs: this is out of the scope of this work and we assume that renewable energy surplus is always available there to fulfil plant power demand, without modeling it.

For each of the A-G cases, we can define an estimate of the OPEX in the three techno-economic scenarios. These values range from 5.12 M€/year of the scenario C.1 (hydropower with optimistic techno-economic hypotheses, i.e., scenario 1) to the upper boundary of 16.8 M€/year of the scenario E.3 (where the system power demand is fulfilled by a CSP plant, under techno-economic assumptions of scenario 3-pessimistic).

Table 12 – Operating costs of the Power-to-MeOH plant

Costs (k€/year)		**Techno-economic scenario**		
		1 – Optimistic	**2 – Realistic**	**3 – Pessimistic**
Fixed OPEX		938	1034	1306
Variable OPEX ($OC_{2+3+5+6+7}$)			181.5	
Scenario for electric energy supply (OC_{1+4})	**A**		5097	
	B		5919	
	C		3864	
	D		6988	
	E		15208	
	F		10441	
	G		4604	

4.3.3. Cost of methanol

Once determined the TIC with the estimates of TOC and OPEX, we computed the cost of methanol (COM), defined as the production cost of methanol that ensures a breakeven over the project lifetime of 25 years (Eq. 19). Considering each source of renewable energy coupled with the plant (cases A-G), we defined a range of COM according to the techno-economic hypotheses presented earlier (scenarios 1-3).

The results are reported in Figure 8, where blue bars represent the range of variation between pessimistic and optimistic scenarios. The values obtained under the realistic techno-economic assumptions (scenario 2) are explicitly reported for the sake of clarity and marked with a blue dot. It is important to remark that this estimation still does not account for the sale of electrolytic oxygen, which is instead vented. We compared the values of COM with the current and the future market price of methanol, 400 €/t and 800 €/t respectively [62].

As expected from the results of Section 4.3.2, case C (hydropower) presents the lowest COM, ranging from 823 to 906 €/t. This range is very close to the predicted price of methanol on future market, hence making this system a competitive configuration for the decarbonization of methanol-based industry and market even without any valorization of electrolytic oxygen.

Five of the considered RES gather in a range that is not far from 800 €/t: in order of increasing price we find hydropower, onshore wind (941-1023 €/t), bioenergy (1019-1101 €/t), geothermal (1150-1232 €/t) and solar PV (1319-1401 €/t). Cases G (onshore wind) and D (solar PV) are of particular interest because they would allow the storage and conversion of large amounts of non-programmable energy generation, hence offering a solution to the abovementioned issues of RES mismatch or, even worse, avoiding its curtailment.

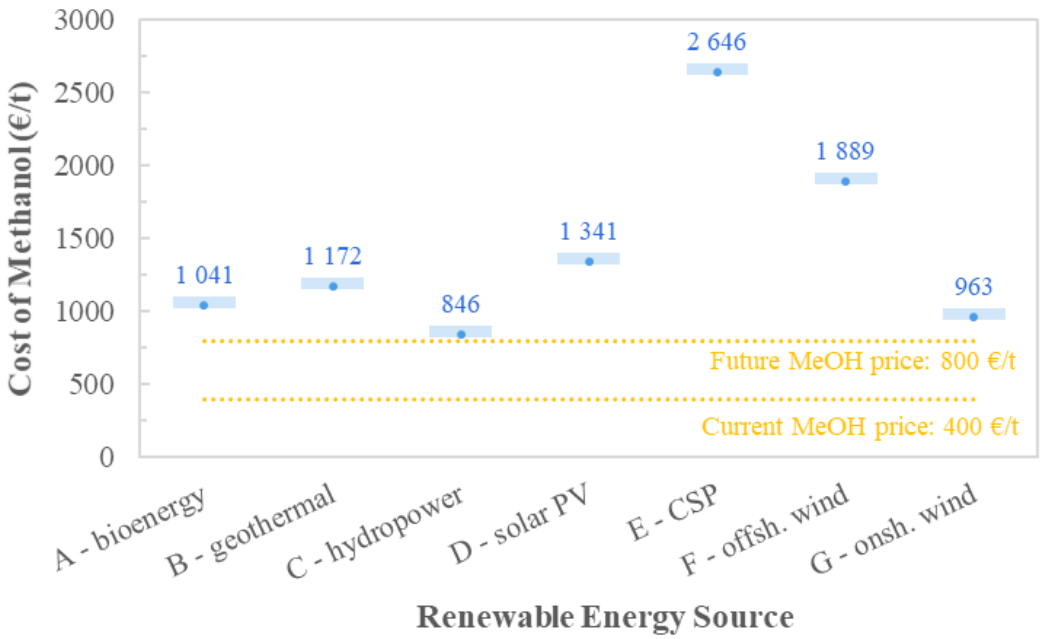

Figure 8 - Variation of COM with the techno-economic scenario and the source of renewable energy

The results obtained strictly depend on the economic assumptions considered. More than others, the cost of electric energy used to run the plant: reductions of this input parameter in the range reported in Table 8 [59] would draw the COM estimates closer to the current methanol price of 400 €/t. For instance, COM would fall under the 1000 €/t threshold whether the lower boundaries of electric energy cost in Table 8 were valid for hydropower (601-684 €/t), onshore wind (785-866 €/t), bioenergy (837-919 €/t), solar PV (967-1049 €/t) geothermal (993-1075 €/t). Case C-hydropower would entirely fall in the 400-800 €/t band, confirming its economic viability under current economic conditions. Finally, a detailed forecasting of the average cost of electric energy would establish the economic competitiveness of these systems in the future methanol market.

The two remaining cases rely on technologies that are still not diffused for commercial application, hence resulting in high values of COM: offshore wind (1867-1949 €/t) and concentrated solar power (2624-2706 €/t). Further demonstration and larger installation would decrease the average cost of electricity from these sources, hence reducing the gap with the cheaper technologies. It is worth remarking that we considered global weighted-average costs in order to be as general as possible without any preference for plant location: local variations of these costs would push up and down the COM confidence bars. However, they represent the least favorable options for this Power-to-MeOH under the current economic conditions. Even considering the lower boundaries of electric energy costs in Table 8, they are too expensive to get a COM smaller than 1600 €/t (i.e. twice the future methanol price of 800 €/t).

4.3.4.Influence of the sale of oxygen from water electrolysis

So far, we have considered methanol as the only product that have a market value. However, oxygen is produced in a great amount as a by-product of water electrolysis (ca. 8 kg per kg of hydrogen). When compressed or liquefied and stored in a tube trailer (with purchasing and operating costs that are neglected in our techno-economic assessment), oxygen can be used for many industrial and manufacturing applications, thus representing a second income in the cash flow analysis.

This section presents our investigation about the effect of the option of selling oxygen on the economic performance of the plant, considering three costs (0-70-150 €/t) in order to span a range for the economic KPIs with enough confidence. The cost of 0 €/t corresponds to the base scenario of oxygen venting.

The income from the sale of oxygen partially counterbalances the OPEX of the plant. In other words, part of the revenues entirely charged on the sale of methanol in Section 4.3.3 can be now allocated to the optional sale of oxygen. The main effect is the reduction of the COM, with the same annual production of methanol (Eq. 19), as shown in Figure 9. For the sake of simplicity, we represented the effect only for the most and the least favorable RES scenarios resulting from Section 4.3.3 (C-hydropower and E-concentrated solar power), with the other configurations being included between these boundaries.

With respect to the values of 824-906 €/t reported in Section 4.3.3 for case C, the COM reduces by 14% (703-784 €/t) and 30% (565-647 €/t) when oxygen is sold at 70 €/t and 150 €/t, respectively. The option of selling oxygen has the beneficial effect of pushing the COM confidence range down in the 400-800 €/t band, between the current and the future market price of methanol. Case C is not only the most viable configuration for the generation of renewable methanol, but would be also competitive with the current "fossil-based" technology chains characterized by an average price that is susceptible to continuous market fluctuations and has overcome the threshold of 400 €/t many times in US and European markets [63] in recent years.

If the cost of electricity in case C was 26.2 €/MWh (lower bound in Table 8), the COM would furtherly reduce to 481-563 €/t (O_2: 70 €/t) and 343-425 €/t (O_2: 150 €/t): in this optimistic – but not unreal – scenario, the cost of the methanol produced by the examined system would be even lower than the average value considered for current market. Similar trends and qualitative results can be expected for the other scenarios of the low-COM block (onshore wind , bioenergy , geothermal , solar PV) identified in Section 4.3.3.

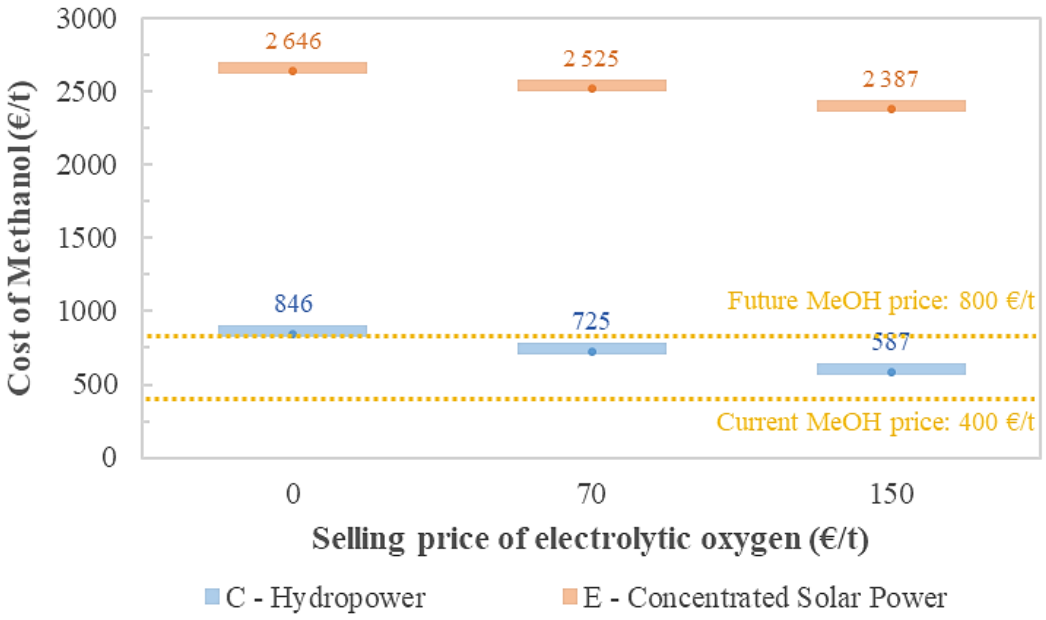

Figure 9 - Effect of the sale of oxygen on the production cost of methanol (COM)

The COM estimates for the cases F-offshore wind and E-concentrated solar power (reported in Figure 9 as red bars) are extremely high. The weight of high-cost electric consumption on the OPEX limits the effect of oxygen sale on the COM reduction with respect to the 2624-2706 €/t in case of venting: -4.5% (O_2: 70 €/t) and -10% (O_2: 150 €/t). Even with the option of oxygen sale as a second income, these configurations keep being out of the methanol market.

4.3.5. Internal Rate of Return: a sensitivity analysis

We finally provide a sensitivity of the main indicator of the investment profitability (i.e., the internal rate of return, IRR) to the techno-economic scenarios (1-optimistic, 2-realistic and 3-pessimistic). In particular, we assessed the levelized cost of methanol (LCOM) ensuring an internal rate of return in the range 0-10% in the two extreme RES configurations (cases C-hydropower and E-concentrated solar power with the respective average values of LCOE in Table 8), considering the option of selling oxygen at different prices: 150 €/t in scenario 1, 70 €/t in scenario 2, 0 €/t in scenario 3.

Figure 10 highlights the results of the sensitivity analysis, with the LCOM associated to IRR = 0% equal to the COM estimated in different scenarios (Figure 9), by definition. As expected, the higher the LCOM, the more profitable the investment is and, hence, the higher the value of the IRR is. What is significant is the comparability

of the LCOM with the future market price of methanol even at very high values of IRR in case C. The lower bound of the blue confidence range in the following figure (corresponding to LCOM in scenario C.1 with oxygen sold at 150 €/t) exceeds 800 €/t at IRR = 8%, a value associated to a very good return performance of the investment. The values of LCOM in realistic scenario (C.2 with oxygen sold at 70 €/t) keep under the threshold of 1000 €/t, except for the value associated to IRR = 10% (1072 €/t).

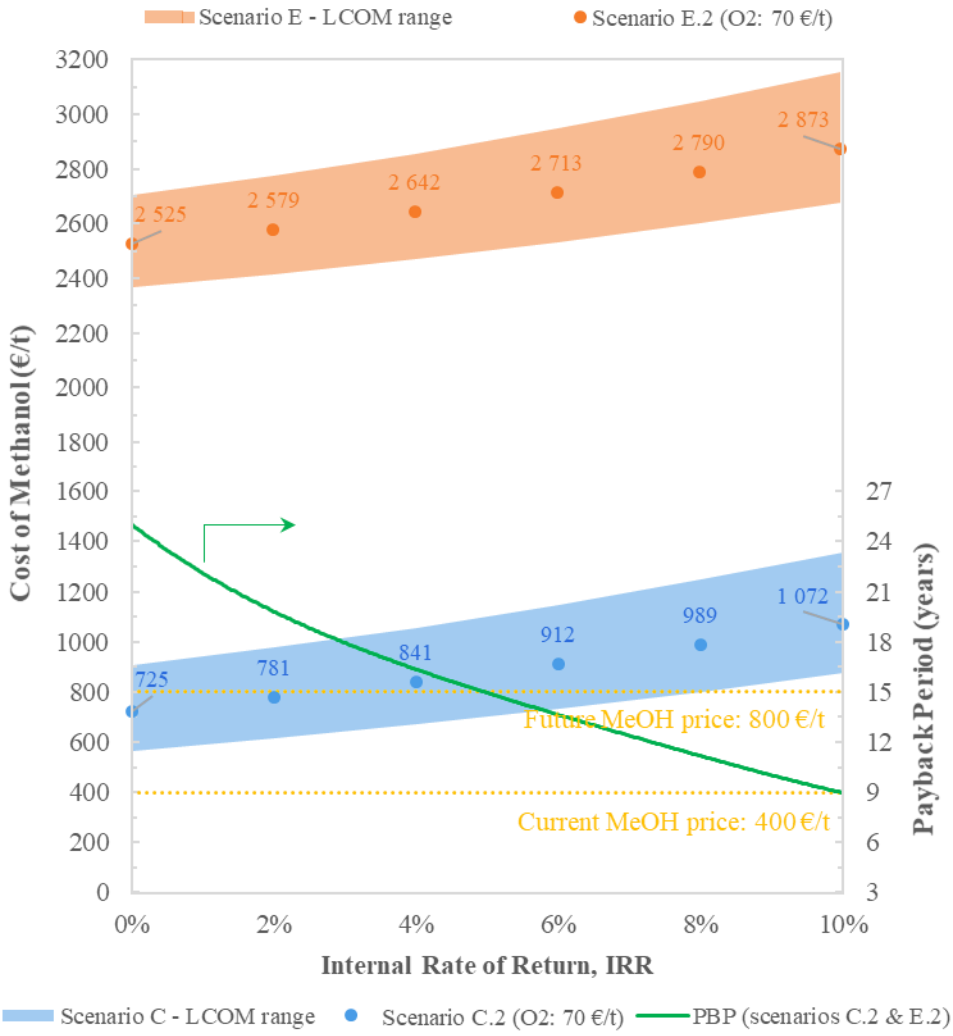

Figure 10 - Variation of the Levelized Cost Of Methanol (left) and Payback Period (right) with the investment internal rate of return in the two extreme scenarios (C-hydropower and E-concentrated solar power)

However, if the cost of electric energy from hydropower was 26.2 €/MWh, the investment IRR would be 10% with

- LCOM = 655 €/t for scenario C.1 with oxygen sold at 150 €/t;
- LCOM = 853 €/t for scenario C.2 with oxygen sold at 70 €/t;
- LCOM = 1135 €/t for scenario C.3 with oxygen vented.

With such IRR, the investment would have an excellent return performance, being extremely competitive in scenarios C.1 and C.2 and with the possibility of a good benefit-cost ratio: if the average discount rate valid during project lifetime was smaller than the IRR, the net present value (NPV) would be strictly positive with certain earnings at the end of plant life.

The results of the sensitivity analysis justify again the option of selling oxygen: its sale determines an average reduction of LCOM of 20% from scenario C.3 (with oxygen venting) to scenario C.1 (O_2: 150 €/t), hence pushing the LCOM confidence range down in the 400-800 €/t band at lower values of IRR.

As expected from the results of LCOM, configuration E is even less competitive if a higher investment IRR is aimed: the prohibitive cost of electric energy would require an excessively high LCOM (2675-2873 €/t at IRR = 10%).

We finally provide the variation of the Payback Period (PBP, Eq. 21) in the different scenarios: green curve (right-hand axis in Figure 10) is provided for scenarios C.2 and E.2 (both with O_2 sold at 70 €/t), but the trend is almost the same for all the other cases. Since the PBP does not account for the discount rate (i.e. the time value of money), the configurations with COM ensuring an IRR = 0% are characterized by a PBP of 25 years, i.e., the project lifetime. Selling methanol at higher COM ensures higher values of IRR and, hence, smaller payback periods: a minimum PBP of 9 years is reached for configurations with IRR = 10%. The graph also provides a qualitative information about the discounted payback time (PBT): if the discount rate was, for instance, 4%, the LCOM should be higher than 841 €/t in scenario C.2 to have a PBT smaller than plant lifetime and a positive NPV. Otherwise, the investment would not return.

Hence, the results of the sensitivity analysis performed can be interpreted as a profitability map for the investment in the Power-to-MeOH plant: for each techno-economic and energy scenario, we provided the indicators of the investment profitability (IRR) and a comparison of the corresponding LCOM with the predicted cost range of the future methanol market, hence outlining the conditions for the system to be competitive.

5. Conclusions

We assessed an integrated system converting about 1.25 t/h of CO_2 captured from a coal-fired power plant into 788 kg/h of methanol through the reaction with "green" hydrogen from water electrolysis (10 MW), following the Power-to-MeOH route. A comprehensive model to simulate the operation of the different sections (water

electrolysis; carbon capture; methanol synthesis) was developed to determine the mass and energy balances of the plant and assess its energy and environmental performance.

- The system ensures an annual reduction of about 10,000 tons of CO_2 with a water consumption of 12.63 * 10^3 m^3/y.
- Heat recovery through the thermal integration of the sections (network of heat exchangers designed in Figure S.1 of the Supplementary Material) can heavily reduce the heating and cooling demand of the plant by 81% and 47%, respectively from the initial values of 5.65 MW and 9.78 MW.
- The specific energy consumption for CO_2 avoided (SPECCA) of 1.26 kWh/kg_{CO2} for the system without thermal integration perfectly agrees with the literature values. Heat recovery through the different sections of the plant allows to reduce dramatically the thermal penalty for the solvent regeneration, hence leaving a residual energy consumption of 0.094 kWh/kg_{CO2} for the carbon capture section.
- The 81% reduction of heating demand thanks to thermal integration allows a strong increase of the system global efficiency from 26.74% to 37.22%, much closer to the value of the Power-to-MeOH gross efficiency (42.48%).

The mass and energy balances resulting from the model simulations were the input for a detailed techno-economic assessment based on a bottom-up approach. From the estimated size of each component, we computed the plant Total Overnight Cost (TOC) under the hypotheses of three economic scenarios: 1-optimistic, 2-realistic, 3-pessimistic. To complete the cash flow analysis, we defined and computed a list of operating costs (OPEX): we assessed their sensitivity to the cost of input electricity introducing seven renewable energy sources (RES) to feed electrolysis and the Balance of Plant (scenarios A-G).

- We estimated a TOC between 27.7 M€ (scenario 1-optimistic) and 40.2 M€ (scenario 3-pessimistic), of which 85-90% can be allocated to the realization of water electrolysis section and the network of recovery heat exchangers for thermal integration.
- The fixed maintenance and insurance costs range from 0.9 to 1.3 M€/y. Variable OPEX are equal to 181.5 k€/y, to which one should sum the cost of feeding the 94.13 GWh/year to run the plant: this contribution ranges from the minimum of 3.86 M€/year in case of hydropower to an upper limit of 15.2 M€/year in case of CSP (concentrated solar power).
- Considering each source of renewable energy coupled with the plant, we defined a confidence range of the cost of methanol (COM) according to the techno-economic hypotheses of scenarios 1-3. Five of the considered RES gather in a range with a COM not far from the future market price of methanol (800 €/t), which are in order of increasing cost: hydropower (823-906 €/t), onshore wind (941-1023 €/t), bioenergy (1019-1101 €/t), geothermal (1150-1232 €/t) and solar PV (1319-1401 €/t). The two remaining scenarios

are characterized by high values of COM: offshore wind (1867-1949 €/t) and concentrated solar power (2624-2706 €/t).

- We investigated the effect of the option of selling oxygen on the economic performance of the plant. With respect to the previous values of 823-906 €/t, the COM in case of hydropower reduces by 14% (703-784 €/t) and 30% (565-647 €/t) when oxygen is sold at 70 €/t and 150 €/t, respectively: selling oxygen has the beneficial effect of pushing the COM confidence range closer to current MeOH market price (400 €/t), improving the competitiveness of the examined system with the traditional methanol synthesis technology chains. Contrarywise, the COM reduction with respect to the 2624-2706 €/t when oxygen venting is limited to -4.5% (O_2: 70 €/t) and -10% (O_2: 150 €/t) in case of concentrated solar power.
- We finally provided a map of the profitability of the investment in the examined Power-to-MeOH plant: we estimated the levelized cost of methanol (LCOM) ensuring an internal rate of return ranging from 0 to 10% for each of the techno-economic scenarios identified. Assuming 10% as the desired IRR, LCOM spans from 874 to 1356 €/t in case of hydropower, hence close to the future market price of MeOH with margin of improvement (655-1135 €/t) in case of lower costs of electric energy from hydropower (26.2 €/MWh). Hence, we proved the techno-economic feasibility of employing "green" methanol as a chemical vector for the decarbonization of process industry even in realistic economic scenarios.

FUNDING

This research did not receive any specific grant from funding agencies in the public, commercial, or not-for-profit sectors.

REFERENCES

[1] World Energy Council, World Energy Scenarios - Exploring innovation pathways to 2040, London, 2019. https://www.worldenergy.org/publications/entry/world-energy-scenarios-2019-european-regional-perspectives.

[2] International Energy Agency, Global Energy & CO_2 Status Report - The latest trends in energy and emissions in 2018, Paris, France, 2019. https://doi.org/10.4324/9781315252056.

[3] United Nations, Paris Agreement on Climate Change, Paris, France - Adopted Dec. 12, 2015; entered into force Nov. 4, 2016, n.d.

[4] IPCC, Global Warming of 1.5°C. An IPCC Special Report on the impacts of global warming of 1.5°C above pre-industrial levels and related global greenhouse gas emission pathways, in the context of strengthening the global

response to the threat of climate change, Geneva, Switzerland, 2018. https://www.ipcc.ch/site/assets/uploads/sites/2/2019/06/SR15_Full_Report_Low_Res.pdf.

[5] G. Buffo, P. Marocco, D. Ferrero, A. Lanzini, M. Santarelli, Power-to-X and Power-to-Power routes, in: Sol. Hydrog. Prod. Process. Syst. Technol., Elsevier, 2019: pp. 530–575. https://doi.org/10.1016/b978-0-12-814853-2.00015-1.

[6] E. Rozzi, F.D. Minuto, A. Lanzini, P. Leone, Green synthetic fuels: Renewable routes for the conversion of non-fossil feedstocks into gaseous fuels and their end uses, Energies. 13 (2020). https://doi.org/10.3390/en13020420.

[7] G. Centi, S. Perathoner, Opportunities and prospects in the chemical recycling of carbon dioxide to fuels, Catal. Today. 148 (2009) 191–205. https://doi.org/10.1016/j.cattod.2009.07.075.

[8] G.A. Olah, A. Goeppert, G.K.S. Prakash, Beyond Oil and Gas: The Methanol Economy, Second, 2009.

[9] The Global CO_2 Initiative - Innovation for Cool Earth Forum, Carbon dioxide utilization (CO_2U) - ICEF Roadmap 1, 2016.

[10] D. Milani, R. Khalilpour, G. Zahedi, A. Abbas, A model-based analysis of CO_2 utilization in methanol synthesis plant, J. CO_2 Util. 10 (2015) 12–22. https://doi.org/10.1016/j.jcou.2015.02.003.

[11] É.S. Van-Dal, C. Bouallou, Design and simulation of a methanol production plant from CO_2 hydrogenation, J. Clean. Prod. 57 (2013) 38–45. https://doi.org/10.1016/j.jclepro.2013.06.008.

[12] O.-S. Joo, K.-D. Jung, I. Moon, A.Y. Rozovskii, G.I. Lin, S.-H. Han, S.-J. Uhm, Carbon Dioxide Hydrogenation To Form Methanol via a Reverse-Water-Gas-Shift Reaction (the CAMERE Process), Ind. Eng. Chem. Res. 38 (1999) 1808–1812. https://doi.org/10.1021/ie9806848.

[13] A.S. Alsuhaibani, S. Afzal, M. Challiwala, N.O. Elbashir, M.M. El-Halwagi, The impact of the development of catalyst and reaction system of the methanol synthesis stage on the overall profitability of the entire plant: A techno-economic study, Catal. Today. 343 (2020) 191–198. https://doi.org/10.1016/j.cattod.2019.03.070.

[14] Science Advice for Policy by European Academies (SAPEA), Novel carbon capture and utilisation technologies, Berlin, Germany, 2018.

[15] X. Xu, Y. Liu, F. Zhang, W. Di, Y. Zhang, Clean coal technologies in China based on methanol platform, Catal. Today. 298 (2017) 61–68. https://doi.org/10.1016/j.cattod.2017.05.070.

[16] C.F. Shih, T. Zhang, J. Li, C. Bai, Powering the Future with Liquid Sunshine, Joule. 2 (2018) 1925–1949. https://doi.org/10.1016/j.joule.2018.08.016.

[17] MefCO_2 Partners, Methanol fuel from CO_2 - Synthesis of methanol from captured carbon dioxide using surplus electricity, (n.d.). http://www.mefco2.eu/ (accessed April 23, 2020).

[18] CORDIS - EU Research Results, MefCO_2 – Synthesis of methanol from captured carbon dioxide using surplus electricity (EU-H2020 - Grant Agreement no. 637016), (n.d.). https://cordis.europa.eu/project/id/637016/ (accessed April 23, 2020).

[19] M. Bowker, Methanol Synthesis from CO_2 Hydrogenation, ChemCatChem. 11 (2019) 4238–4246. https://doi.org/10.1002/cctc.201900401.

[20] CRI - Carbon Recycling International, Projects - Emissions-to-liquids technologies, (n.d.). https://www.carbonrecycling.is/projects#project-goplant/ (accessed April 23, 2020).

[21] C. Hobson, C. Márquez, Renewable Methanol Report, Madrid, Spain, 2018. www.methanol.orgwww.methanol.org.

[22] The Global CO_2 Initiative - Innovation for Cool Earth Forum, Carbon dioxide utilization (CO_2U) - ICEF Roadmap 2, 2017. https://doi.org/10.1017/CBO9781107415324.004.

[23] L. Wang, M. Chen, R. Küngas, T.E. Lin, S. Diethelm, F. Maréchal, J. Van herle, Power-to-fuels via solid-oxide electrolyzer: Operating window and techno-economics, Renew. Sustain. Energy Rev. 110 (2019) 174–187. https://doi.org/10.1016/j.rser.2019.04.071.

[24] J. Nyári, M. Magdeldin, M. Larmi, M. Järvinen, A. Santasalo-Aarnio, Techno-economic barriers of an industrial-scale methanol CCU-plant, J. CO_2 Util. 39 (2020). https://doi.org/10.1016/j.jcou.2020.101166.

[25] K. Atsonios, K.D. Panopoulos, E. Kakaras, Investigation of technical and economic aspects for methanol production through CO_2 hydrogenation, Int. J. Hydrogen Energy. 41 (2016) 2202–2214. https://doi.org/10.1016/j.ijhydene.2015.12.074.

[26] D. Bellotti, M. Rivarolo, L. Magistri, A.F. Massardo, Feasibility study of methanol production plant from hydrogen and captured carbon dioxide, J. CO_2 Util. 21 (2017) 132–138. https://doi.org/10.1016/j.jcou.2017.07.001.

[27] G. Iaquaniello, G. Centi, A. Salladini, E. Palo, S. Perathoner, L. Spadaccini, Waste-to-methanol: Process and economics assessment, Bioresour. Technol. 243 (2017) 611–619. https://doi.org/10.1016/j.biortech.2017.06.172.

[28] M. Pérez-Fortes, J.C. Schöneberger, A. Boulamanti, E. Tzimas, Methanol synthesis using captured CO_2 as raw material: Techno-economic and environmental assessment, Appl. Energy. 161 (2016) 718–732. https://doi.org/10.1016/j.apenergy.2015.07.067.

[29] R. Notz, H.P. Mangalapally, H. Hasse, Post combustion CO_2 capture by reactive absorption: Pilot plant description and results of systematic studies with MEA, Int. J. Greenh. Gas Control. 6 (2012) 84–112. https://doi.org/10.1016/j.ijggc.2011.11.004.

[30] F. Calogero, Methanol synthesis through CO_2 hydrogenation: reactor and process modelling (M.Sc. thesis), Politecnico di Torino, 2018. https://webthesis.biblio.polito.it/9229/1/tesi.pdf.

[31] G. Latini, M. Signorile, V. Crocellà, S. Bocchini, C.F. Pirri, S. Bordiga, Unraveling the CO_2 reaction mechanism in bio-based amino-acid ionic liquids by operando ATR-IR spectroscopy, Catal. Today. 336 (2019) 148–160. https://doi.org/10.1016/j.cattod.2018.12.050.

[32] D.W. Keith, G. Holmes, D. St. Angelo, K. Heidel, A Process for Capturing CO_2 from the Atmosphere, Joule. 2 (2018) 1573–1594. https://doi.org/10.1016/j.joule.2018.05.006.

[33] M.E. Boot-Handford, J.C. Abanades, E.J. Anthony, M.J. Blunt, S. Brandani, N. Mac Dowell, J.R. Fernández, M.C. Ferrari, R. Gross, J.P. Hallett, R.S. Haszeldine, P. Heptonstall, A. Lyngfelt, Z. Makuch, E. Mangano, R.T.J. Porter, M. Pourkashanian, G.T. Rochelle, N. Shah, J.G. Yao, P.S. Fennell, Carbon capture and storage update, Energy Environ. Sci. 7 (2014) 130–189. https://doi.org/10.1039/c3ee42350f.

[34] R. Raudaskoski, E. Turpeinen, R. Lenkkeri, E. Pongrácz, R.L. Keiski, Catalytic activation of CO_2: Use of secondary CO_2 for the production of synthesis gas and for methanol synthesis over copper-based zirconia-containing catalysts, Catal. Today. 144 (2009) 318–323. https://doi.org/10.1016/j.cattod.2008.11.026.

[35] R. Gaikwad, A. Bansode, A. Urakawa, High-pressure advantages in stoichiometric hydrogenation of carbon dioxide to methanol, J. Catal. 343 (2016) 127–132. https://doi.org/10.1016/j.jcat.2016.02.005.

[36] F. Liao, X.-P. Wu, J. Zheng, M.M.-J. Li, A. Kroner, Z. Zeng, X. Hong, Y. Yuan, X.-Q. Gong, S.C.E. Tsang, A promising low pressure methanol synthesis route from CO_2 hydrogenation over Pd@Zn core–shell catalysts, Green Chem. 19 (2017) 270–280. https://doi.org/10.1039/C6GC02366E.

[37] F. Studt, I. Sharafutdinov, F. Abild-Pedersen, C.F. Elkjær, J.S. Hummelshøj, S. Dahl, I. Chorkendorff, J.K. Nørskov, Discovery of a Ni-Ga catalyst for carbon dioxide reduction to methanol, Nat. Chem. 6 (2014) 320–324. https://doi.org/10.1038/nchem.1873.

[38] J.A. Singh, A. Cao, J. Schumann, T. Wang, J.K. Nørskov, F. Abild-Pedersen, S.F. Bent, Theoretical and Experimental Studies of CoGa Catalysts for the Hydrogenation of CO_2 to Methanol, Catal. Letters. 148 (2018) 3583–3591. https://doi.org/10.1007/s10562-018-2542-x.

[39] M. Gamba, Renewable Electricity Storage: techno-economic assessment and Power-to-Power options (M.Sc. Thesis), Politecnico di Torino, 2016.

[40] A. Ursúa, L.M. Gandía, P. Sanchis, Hydrogen production from water electrolysis: Current status and future trends, Proc. IEEE. 100 (2012) 410–426. https://doi.org/10.1109/JPROC.2011.2156750.

[41] M. Götz, J. Lefebvre, F. Mörs, A. McDaniel Koch, F. Graf, S. Bajohr, R. Reimert, T. Kolb, Renewable Power-to-Gas: A technological and economic review, Renew. Energy. 85 (2016) 1371–1390. https://doi.org/10.1016/j.renene.2015.07.066.

[42] R. Canepa, M. Wang, C. Biliyok, A. Satta, Thermodynamic analysis of combined cycle gas turbine power plant with post- combustion CO_2 capture and exhaust gas recirculation, J. Process Mech. Eng. 227 (2012) 89–105. https://doi.org/10.1177/0954408912469165.

[43] S. Moioli, L.A. Pellegrini, S. Gamba, Simulation of CO_2 capture by MEA scrubbing with a rate-based model, Procedia Eng. 42 (2012) 1651–1661. https://doi.org/10.1016/j.proeng.2012.07.558.

[44] W.K. Lewis, W.G. Whitman, Principles of Gas Absorption, Ind. Eng. Chem. 16 (1924) 1215–1220. https://doi.org/10.1021/ie50180a002.

[45] Y. Huang, X. Zhang, X. Zhang, H. Dong, S. Zhang, Thermodynamic Modeling and Assessment of Ionic Liquid-

Based CO_2 Capture Processes, Ind. Eng. Chem. Res. 53 (2014) 11805–11817. https://doi.org/10.1021/ie501538e.

[46] B. Zacchello, E. Oko, M. Wang, A. Fethi, Process simulation and analysis of carbon capture with an aqueous mixture of ionic liquid and monoethanolamine solvent, Int. J. Coal Sci. Technol. 4 (2017) 25–32. https://doi.org/10.1007/s40789-016-0150-1.

[47] T.E. Akinola, E. Oko, M. Wang, Study of CO_2 removal in natural gas process using mixture of ionic liquid and MEA through process simulation, Fuel. 236 (2019) 135–146. https://doi.org/10.1016/j.fuel.2018.08.152.

[48] B. Baburao, S. Bedell, P. Restrepo, D. Schmidt, C. Schubert, B. Debolt, I. Haji, F. Chopin, Advanced Amine Process Technology Operations and Results from Demonstration Facility at EDF Le Havre, Energy Procedia. 63 (2014) 6173–6187. https://doi.org/10.1016/j.egypro.2014.11.649.

[49] J.N. Knudsen, J.N. Jensen, P. Vilhelmsen, O. Biede, Experience with CO_2 capture from coal flue gas in pilot-scale: Testing of different amine solvents, Energy Procedia. 1 (2009) 783–790. https://doi.org/10.1016/j.egypro.2009.01.104.

[50] G.H. Graaf, J.G.M. Winkelman, Chemical Equilibria in Methanol Synthesis Including the Water-Gas Shift Reaction: A Critical Reassessment, Ind. Eng. Chem. Res. 55 (2016) 5854–5864. https://doi.org/10.1021/acs.iecr.6b00815.

[51] National Energy Technology Laboratory (NETL), Cost Estimation Methodology for NETL Assessments of Power Plant Performance, 2019. http://www.netl.doe.gov/File Library/research/energy analysis/publications/QGESSNETLCostEstMethod.pdf.

[52] R. Turton, R. Bailie, W. Whiting, J. Shaeiwitz, Analysis, Synthesis, and Design of Chemical Processes, 3rd ed., Pearson Education, Inc., Boston, USA, 2009.

[53] Global CCS Institute, Economic Assessment of Carbon Capture and Storage Technologies: 2011 Update, Canberra, Australia, 2011. https://www.globalccsinstitute.com/archive/hub/publications/12786/economic-assessment-carbon-capture-and-storage-technologies-2011-update.pdf.

[54] D. Voldsund, Mari Anantharaman, Rahul Berstad, E. De Lena, C. Fu, S. Gardarsdottir, A. Jamali, J.-F. Pérez-Calvo, O. Romano, Matteo Roussanaly, Simon Ruppert, Johannes Stallmann, D. Sutter, CEMCAP - Comparative techno-economic analysis of CO_2 capture in cement plants (deliverable 4.6), 2018. https://doi.org/10.5281/zenodo.2597091.

[55] D.S. Remer, L.H. Chai, Process Equipment, Cost Scale-up, in: J. McKetta (Ed.), Encycl. Chem. Process. Des., 43rd ed., 1993: pp. 306–317. https://scholarship.claremont.edu/hmc_fac_pub/789/.

[56] Chemical Engineering, 2019 Chemical Engineering Plant Cost Index Annual Average, (2020). https://www.chemengonline.com/2019-chemical-engineering-plant-cost-index-annual-average/ (accessed September 24, 2020).

[57] J. Proost, State-of-the art CAPEX data for water electrolysers, and their impact on renewable hydrogen price settings, Int. J. Hydrogen Energy. 44 (2019) 4406–4413. https://doi.org/10.1016/j.ijhydene.2018.07.164.

[58] M.F. Shehzad, M.B. Abdelghany, D. Liuzza, V. Mariani, L. Glielmo, Mixed logic dynamic models for MPC control of wind farm hydrogen-based storage systems, Inventions. 4 (2019) 1–17. https://doi.org/10.3390/inventions4040057.

[59] International Renewable Energy Agency (IRENA), Renewable power generation costs in 2018, Abu Dhabi, 2019.

[60] J. Kärki, E.V. Lut, Screening for the most promising business cases for P2X deployment in renewable energy systems, 2017.

[61] M. Hurskainen, Industrial oxygen demand in Finland (VTT-R-06563-17), Jyväskylä, Finland, 2017. www.neocarbonenergy.fi.

[62] D. Bellotti, M. Rivarolo, L. Magistri, Economic feasibility of methanol synthesis as a method for CO_2 reduction and energy storage, Energy Procedia. 158 (2019) 4721–4728. https://doi.org/10.1016/j.egypro.2019.01.730.

[63] Methanex, Historical Methanex Posted Price, (n.d.). https://www.methanex.com/our-business/pricing/ (accessed July 30, 2020).